Energetics of Two-level Shears and Hardening of Single Crystals

LUCA DESERI
Dipartimento di Ingegneria, Universit di Ferrara, 44100 Ferrara, Italy

DAVID R. OWEN[1]
Department of Mathematical Sciences, Carnegie Mellon University, Pittsburgh, PA 15213, USA

(Received 22 March 2001; Final version 2 November 2001)

Abstract: An energetic description of the hardening behavior of single crystals undergoing single slip is analyzed. Simultaneous macroscopic simple shear and mesoscopic slips are described by means of a class of structured deformations called "two-level shears," along with recently proposed measures of separation of active slip-bands and the number of lattice cells traversed during slip. The energetics of two-level shears gives rise to a response consistent with the experimentally observed loading and unloading behavior of a single crystal in G. I. Taylor's soft device, as well as with the Portevin–le Chatelier effect. The initial critical resolved shear stress, the flow stress, and the hardening response are obtained, and an application to aluminum single crystals is discussed.

1. INTRODUCTION

Pioneering experimental and theoretical studies of the distortion of single crystals were performed by G. I. Taylor and his co-workers beginning in the 1920s [1]. More recently, theories of plasticity [2, 3] have been adapted to model single crystals undergoing finite deformations [4, 5]. In these studies, quantities associated with slip mechanisms are taken in addition to the gradient of the macroscopic deformation in order to describe sub-macroscopic geometrical changes, and the additional quantities play the role of internal variables in the constitutive relations. In a recent paper [6], an energetic approach, in which plastic deformation is introduced by means of an internal variable provides detailed information on geometrical changes experienced by single crystals undergoing multiple slip.

The present research is an initial step toward determining the suitability of the recent theory of structured deformations of continua [7–9] for describing the hardening behavior of single crystals. The theory of structured deformations permits the systematic incorporation of geometrical changes at more than one length scale into continuum theories without the introduction of internal variables. In this first attempt to describe hardening in terms of structured deformations, we employ for the sake of simplicity a particular family of structured deformations called two-level shears [10]. Each of these non-classical deformations is characterized by a pair of orthogonal unit vectors and by two numbers μ and γ that are shown to be the macroscopic shear and the shear without slip, respectively. Two-level shears describe not only slips that occur in one crystallographic direction along narrow slip bands parallel to a single family of slip planes, but also lattice distortions that occur away from the slip

Mathematics and Mechanics of Solids, **7:** 113–147, 2002

bands. In addition, these special structured deformations incorporate through the number $\mu - \gamma$ the effects at the macrolevel of slips along individual slip bands at the mesolevel, and the present study may be viewed as a meso-macroscale energetic model of hardening in the special context of two-level shears. A broader energetic model based on structured deformations that treats multiple slip in an incremental context is currently under study, while an incremental description of multiple slip without energetics and based on structured deformations is available in [11].

The reference configuration of the continuous body that we consider reflects the geometry of the samples of single crystals that G. I. Taylor used in his experiments on aluminum and other crystals undergoing slip [1]. Following Taylor, we take the magnitude of the applied force to be prescribed on the top and on the bottom faces of a single crystal, with the tractions on the lateral faces of the crystal taken to be zero. The macroscopic deformation of the sample and the boundary conditions can be described completely in terms of the macroshear μ, the orientation of the crystallographic axes in the reference configuration, the orientation of the slip direction in the slip plane, and the magnitude of the applied force. We show that a state of constant stress is compatible with the assumed boundary conditions and with the geometry of deformation; moreover balance of forces and moments are satisfied. For the case of tensile loading, we recover Taylor's formula for the shear component τ of the traction on a slip plane, resolved in the direction of slip (*resolved shear stress*). According to this formula, τ is a monotonic function of the macroshear μ and depends on the magnitude of the applied force and the orientation of the crystallographic axes. The graph of τ versus μ will be called the *load–orientation* curve.

The shear without slip γ for a given two-level shear plays no role up to this point. In particular, the distribution of the macroshear μ between shear without slip γ and shear due to slip $\mu - \gamma$ is not restricted by the considerations above. A prescription of the constitutive relations of the material is required in order to determine this distribution. Here, we provide constitutive relations at a material point by seeking local minimizers of the Gibbs free energy density $\mathcal{E}(\mu, \gamma\,; f) = \Psi(\mu, \gamma) - w(\mu; f)$ in a body that undergoes the two-level shear under the prescribed tensile load f. In this formula for $\mathcal{E}(\mu, \gamma\,; f)$, the term $\Psi(\mu, \gamma)$ is the Helmholtz free energy per unit reference volume, and $w(\mu; f)$ is the work done per unit volume by the tractions produced by the tensile load f. Our principal constitutive relation complies with the general form of free energies for structured deformations [12] and rests on the analysis [13] of the role of active slip-band separation in the energetics of single crystals. These considerations lead to the following additive decomposition for the free energy density:

$$\Psi(\mu, \gamma) = \varphi(\gamma) + p\psi_1\left(\frac{1}{p}\int_0^{\mu-\gamma} \mathfrak{h}(r)dr\right).$$

The first term $\varphi(\gamma)$ represents the energy due to distortion of the crystalline lattice, with φ a smooth, convex function. The second term represents the energy due to the relative translation of adjacent pieces of the lattice along the active slip bands in the crystal, and ψ_1 is a bounded, periodic function with period one. For most of the analysis in this paper, the function $\mathfrak{h}$ in the argument of ψ_1 is taken to be continuous, non-decreasing, and satisfying $\mathfrak{h}(0) = 1$.

Previous analysis [10] of the above formula for Ψ was restricted to the case $\mathfrak{h}(s) = 1$ for all $s \geq 0$, although both tensile and compressive loads were considered there. The term containing ψ_1 reduces in [10] to $p\psi_1(\frac{\mu-\gamma}{p})$ and reflects the periodicity of the crystalline lattice away from slip-bands [2]. The dimensionless number p in the formula for Ψ is identified in [10] with the ratio of one atomic distance to the spacing of active slip-bands in the crystal, measured in atomic distances, and is of the order 10^{-4} in many crystals. The constitutive equation resulting from the process of finding local minimizers of the corresponding Gibbs free energy was shown in [10] to exhibit elastic-perfectly plastic behavior with yield stress $\tau_y = \max \psi_1'$. In the $\mu-\tau$ plane the metastable branches of the constitutive locus correspond to local minimizers (μ, γ) of the Gibbs free energy, are congruent to one another, and are separated from one another by an amount p in the μ-direction. The particular type of yielding and dissipation associated with elastic-perfectly plastic behavior arises automatically in this energetic description through material instabilities at the mesoscale. These instabilities permit a point $(\mu, \pm\tau_y)$ at the end of one metastable branch to jump to a point of the form $(\mu + jp, \pm\tau_y)$ at the end of another metastable branch, with j a positive integer if $\tau = +\tau_y$ and a negative integer if $\tau = -\tau_y$. These jumps in μ (as well as in $\mu - \gamma$) are shown in [10] to be irreversible and to correspond to what is usually called "plastic deformation" or, in the context of single crystals, "irreversible slip". Reversible loading and unloading behavior also are outcomes of the energetic analysis in [10], but no hardening effect is captured. In a precise sense described in [10], the deforming crystal at the mesolevel is like a deck of cards in which individual cards each can shear and can slip relative their neighbors.

Here, we treat in detail the case where $\mathfrak{h}$ is not the constant function 1. This relaxing of the restriction $\mathfrak{h}(s) = 1$ for all s now permits the deforming crystal at the mesolevel to be like a deck of cards that, in addition to experiencing shears and slips of individual cards, can have individual cards becoming thicker as the deformation progresses. For a fixed magnitude f of the load per unit area on the ends of a crystal, we obtain the local minimizers (μ, γ) of the Gibbs free energy $\mathcal{E}$. We show that, as f varies, the local minimizers form an infinite family of non-intersecting, metastable branches that increase in size but decrease in separation as $\mu - \gamma$ increases. Moreover, an end of each of these metastable branches is reached when f reaches a value, called a threshold load, for which the corresponding load–orientation curve is tangent to the metastable branch. An argument similar to ones presented in Sections 6 and 10 shows that the locus of unstable points that form the ends of metastable branches is well depicted by the envelope of the metastable branches taken with respect to the parameter p. When the function φ is quadratic, the envelope has the same shape as the graph of the function $\mathfrak{h}$. In these energetic considerations, two-level shears compatible with a given threshold load f are characterized by a discrete set of points in the $\mu - \tau$ plane: these points correspond to local minima of $\mathcal{E}$ on the load–orientation curve for the given number f, and they always lie on or below the envelope. We show that the jumps in the slip from an endpoint of a metastable branch to a neighboring metastable branch result in a reduction of the Gibbs free energy $\mathcal{E}$, and our model also delimits the two-level shears that may occur as the tensile load is removed.

In Section 2 we recall the principal constitutive assumptions made in [13] relating the separation of active slip-bands to the shear due to slip, and relating the Helmholtz free energy to the shear due to slip $\mu - \gamma$ and to the shear without slip γ. Section 3 contains a description of Taylor's soft device and the corresponding load–orientation curves that relate the resolved shear stress to the applied load and to the orientation of the crystal. In Section 4 we determine

both the local minimizers of the Gibbs free energy of a material element of the crystal as well as the constitutive curve in the $\mu - \tau$ plane, and we analyze the threshold points at which material instabilities at the mesolevel can arise. The response of the crystal in Taylor's soft device to monotonically increasing loads is studied in detail in Section 5, and we show there that the metastable points (μ, τ) compatible with such loading form a "staircase" locus similar to ones observed and usually referred to in connection with the "Portevin–le Chatelier effect". The initial critical resolved shear stress τ_c is identified in Section 6 as the constitutive quantity $\max \psi_1'$ and is shown there to be the limit of shear stresses corresponding to the smallest threshold loads as the initial relative separation of active slip-bands tends to infinity. In Section 7 we show that the envelope of the constitutive curve is determined explicitly by the initial critical shear stress τ_c and by the functions $\mathfrak{h}$ and φ. We show that all of the points on the constitutive curve and, hence, all of the "staircase" loading points must lie on or below the envelope, and we identify the flow stress as a function of the shear due to slip. In Section 8 we discuss unloading of the crystal, and in Section 9 we determine from Taylor's data and measured values of τ_c for aluminum single crystals a formula for the envelope and for the dependence of the relative separation of active slip-bands on the slip.

2. HELMHOLTZ FREE ENERGY

We assume that the crystal undergoes a two-level shear specified by giving two numbers μ, the macroscopic shear, and γ, the shear without slip, along with other quantities to be introduced in Section 3. For the sake of simplicity, we follow [10] and take the macroscopic shear and the shear without slip to be constant throughout the crystal.

Theorems in the theory of structured deformations [7, 8] tell us that for each two-level shear, there exists a sequence $k \mapsto \mathbf{f}_k$ of piecewise-affine deformations such that

$$s := \mu - \gamma = \lim_{r\to 0} \lim_{k\to\infty} \frac{\displaystyle\int_{\mathcal{B}(x;r)\cap\Gamma(\mathbf{f}_k)} [f_k](y)\,dA_y}{vol\mathcal{B}(x;r)}, \tag{2.1}$$

where $\Gamma(\mathbf{f}_k)$ is a family of parallel planes on which $\mathbf{f}_k$ has only tangential jump discontinuities, $[f_k](y)$ is the component of the jump in $\mathbf{f}_k$ in the direction of the jump at a point $y \in \Gamma(\mathbf{f}_k)$, and $\mathcal{B}(x;r)$ is the ball of radius r centered at x, a fixed but arbitrary point in the body. The formula (2.1) permits us to identify the difference $s = \mu - \gamma$ between the macroshear μ and the shear without slip γ as the *shear due to slip*. We interpret each plane in the family $\Gamma(\mathbf{f}_k)$ as an active slip band and each jump $[f_k](y)$ as a displacement of the crystal on one side of the slip band relative to the opposite side. Typically, the number of planes in the jump set $\Gamma(\mathbf{f}_k)$ of $\mathbf{f}_k$ tends to infinity and their separation, as well as the jumps $[f_k](y)$, tends to zero as k tends to infinity.

Let c_k be a positive number that represents the cell-size of the crystal lattice associated with the index k, and define

$$d_k(x;r) := \frac{1}{c_k} \frac{vol\mathcal{B}(x;r)}{area\,(\mathcal{B}(x;r)\cap\Gamma(\mathbf{f}_k))}, \tag{2.2}$$

the (*non-dimensionalized*) *average separation of the active slip bands for the index* k. We assume that both the cell-size c_k and the fraction $\frac{vol\mathcal{B}(x;r)}{area(\mathcal{B}(x;r)\cap\Gamma(\mathbf{f}_k))}$, the (dimensional) average spacing of active slip bands, tend to zero as k tends to infinity and as r tends to zero in such a way that the limit

$$d(x) := \lim_{r\to 0}\lim_{k\to\infty} d_k(x;r) \tag{2.3}$$

exists and is non-zero. The number $d(x)$ represents the *separation of active slip bands relative to the lattice cell-size at* x, and, following the physical motivation presented in [14] and the analysis in [13], we are led to the assumption that $d(x)$ *is determined in each two-level shear by the shear due to slip* $s = \mu - \gamma$:

$$d(x) = \hat{d}(s), \tag{2.4}$$

with $\hat{d}$ a smooth function. As we noted in [13], the product $sd(x)$ is given by the formula

$$sd(x) = \lim_{r\to 0}\lim_{k\to\infty} \frac{\displaystyle\int_{\mathcal{B}(x;r)\cap\Gamma(\mathbf{f}_k)} ([f_k](y)/c_k)\, dA_y}{area\,(\mathcal{B}(x;r)\cap\Gamma(\mathbf{f}_k))} \tag{2.5}$$

and so represents an average with respect to area of non-dimensional tangential jumps. Thus, by (2.4) and (2.5), not only is the separation $d(x)$ of active slip bands relative to the lattice spacing determined by the shear due to slip s, but so also is the average non-dimensional tangential jump $sd(x)$:

$$sd(x) = s\hat{d}(s). \tag{2.6}$$

An important distinction between the two dimensionless quantities s and $s\hat{d}(s)$ now emerges: the number s, by (2.1), represents the amount of shear due to tangential jumps, while the number $s\hat{d}(s)$, by (2.3) and (2.4), measures the average number (possibly fractional) of lattice cells traversed during this shearing.

The main energetic constitutive assumption studied in [13] leads to the condition that, in a two-level shear with macroshear μ and shear without slip γ, the volume density of Helmholtz free energy due to slip $\mathcal{H}^s$ is determined by $(\mu-\gamma)\hat{d}(\mu-\gamma)$, the average number of lattice cells traversed in the two-level shear. In stating this condition explicitly, it is convenient to use $\hat{d}(0)$, the relative separation of active slip-bands at $s = 0$, as a normalization constant, and we write:

$$\mathcal{H}^s = \frac{1}{\hat{d}(0)}\psi_1((\mu-\gamma)\hat{d}(\mu-\gamma)), \tag{2.7}$$

where ψ_1 is a periodic function of period 1. Note that if the separation $\hat{d}(s)$ is frozen at a value $\hat{d}(s_0)$ and an additional slip of amount $\frac{i}{\hat{d}(s_0)}$ occurs, with i an integer, then the periodicity of ψ_1 tells us that

$$\psi_1\left(\left(s_0+\frac{i}{\hat{d}(s_0)}\right)\hat{d}(s_0)\right)=\psi_1(s_0\hat{d}(s_0)+i)=\psi_1(s_0\hat{d}(s_0)). \tag{2.8}$$

Hence, when the distribution of active slip bands is frozen, the additional slips of amount $\frac{i}{\hat{d}(s_0)}$ do not change $\mathcal{H}^s$ and can be considered as being undetected by the crystal. Moreover, by (2.2)–(2.4),

$$\begin{aligned}\frac{i}{\hat{d}(s_0)} &= i\lim_{r\to 0}\lim_{k\to\infty}\frac{c_k\,area\,(\mathcal{B}(x;r)\cap\Gamma(\mathbf{f}_k))}{vol\,\mathcal{B}(x;r)}\\ &= \lim_{r\to 0}\lim_{k\to\infty}\frac{\displaystyle\int_{\mathcal{B}(x;r)\cap\Gamma(\mathbf{f}_k)} ic_k\,dA_y}{vol\,\mathcal{B}(x;r)}\end{aligned} \tag{2.9}$$

and, by (2.1), we conclude that $\frac{i}{\hat{d}(s_0)}$ represents the shear due to tangential jumps of amount i lattice cells. Thus, our constitutive relation (2.7) implies that the free energy density due to slip is not affected by tangential jumps across an integral number of lattice cells when the separation of active slip bands is frozen.

We put

$$\mathfrak{h}(s):=\frac{d}{ds}\left(\frac{s\hat{d}(s)}{\hat{d}(0)}\right) \tag{2.10}$$

and note that relation (2.7) now can be rewritten as

$$\mathcal{H}^s=p\psi_1(\frac{1}{p}\int_0^{\mu-\gamma}\mathfrak{h}(r)dr), \tag{2.11}$$

where $p:=\frac{1}{\hat{d}(0)}$ represents the shear due to tangential jumps across one lattice cell when $s=0$.

Our constitutive description of the Helmholtz free energy density is completed with a specification of the contribution $\mathcal{H}^d$ from the lattice distortions, i.e., the shear without slip γ . From the analysis in [13], we assume that in a two-level shear

$$\mathcal{H}^d=\varphi(\gamma) \tag{2.12}$$

where φ is a non-negative convex function. We now assume that the Helmholtz free energy density $\mathcal{H}$ in a two-level shear is given by

$$\mathcal{H}=\mathcal{H}^s+\mathcal{H}^d. \tag{2.13}$$

By relations (2.11) and (2.12), the Helmholtz free energy density $\mathcal{H}=\Psi(\mu,\gamma)$ for a two-level shear then is given by

$$\Psi(\mu,\gamma) = \varphi(\gamma) + p\psi_1\left(\frac{1}{p}\int_0^{\mu-\gamma} \mathfrak{h}(r)dr\right). \tag{2.14}$$

We also assume from now on that the function $\mathfrak{h}$ defined in (2.10) is a non-decreasing function of s for $s \geq 0$. Therefore, by (2.10),

$$\mathfrak{h}(s) = \frac{\hat{d}(s)}{\hat{d}(0)} + s\frac{\hat{d}'(s)}{\hat{d}(0)},$$

so that $\mathfrak{h}(0) = 1$ and

$$\mathfrak{h}(s) \geq \mathfrak{h}(0) = 1. \tag{2.15}$$

Moreover, because slip bands are separated by at least one lattice cell, we may assume that $\hat{d}(s) \geq 1$ for all $s \geq 0$. We note without proof that $\mathfrak{h}$ is a constant function if and only if $\hat{d}$ is a constant function and that the assumed monotonicity of $\mathfrak{h}$ is equivalent to monotonicity of $\hat{d}$.

If the separation of active slip bands does not vary with the amount of slip, then $\hat{d}(s) = \hat{d}(0)$, $\mathfrak{h}(s) = \mathfrak{h}(0) = 1$ for all s, and relation (2.7) and the definition $p = \hat{d}(0)^{-1}$ yield

$$\Psi(\mu,\gamma) = \varphi(\gamma) + p\psi_1\left(\frac{\mu-\gamma}{p}\right). \tag{2.16}$$

The mapping $s \mapsto \psi(s) := p\psi_1(\frac{s}{p})$ is a periodic function with period p. Thus, when the separation of active slip bands does not vary, the Helmholtz free energy due to slip is a periodic function of the shear due to slip whose period is the reciprocal of the (constant) relative separation of active slip bands. The formula (2.16) was the starting point of the analysis of hysteresis, dissipation, and yielding in the study [10], where the separation of active slip bands was assumed to be a constant of the order 10^4 lattice cell-sizes, so that the period p was of the order 10^{-4}.

3. TAYLOR'S SOFT DEVICE FOR TENSILE LOADING

We consider a single crystal that in its reference configuration occupies a cylindrical region $\mathcal{C}_R := \Omega_R \times (0, \ell_R)$, with $\ell_R > 0$ the height of the crystal and with $\Omega_R \subset \mathbb{R}^2$ a bounded region representing the constant cross-section of the crystal. The common direction of the generators of $\mathcal{C}_R$ is given by the unit vector $\mathbf{e}_3$. If Ω_R^+ and Ω_R^- are the top and bottom faces of the crystal, with outer normals $\mathbf{e}_3$ and $-\mathbf{e}_3$, respectively, then the boundary $\partial\mathcal{C}_R$ of $\mathcal{C}_R$ is given by the formula $\partial\mathcal{C}_R = \Omega_R^+ \cup \Omega_R^- \cup (\partial\Omega_R \times (0, \ell_R))$.

Taylor ([1], p.212) assumed as reference parameters for experimental observations of crystals the angle θ_0 between a slip plane with unit normal $\mathbf{n}$ and the top face of the crystal, i.e., the angle between the vectors $\mathbf{n}$ and $\mathbf{e}_3$, and the angle η_0 between the direction of slip $\mathbf{m}$ and the direction of greatest slope in the slip plane. If $\mathbf{d}$ denotes a unit vector in this direction, then $\cos\eta_0 = \mathbf{d}\cdot\mathbf{m}$ (see Figure 1) and

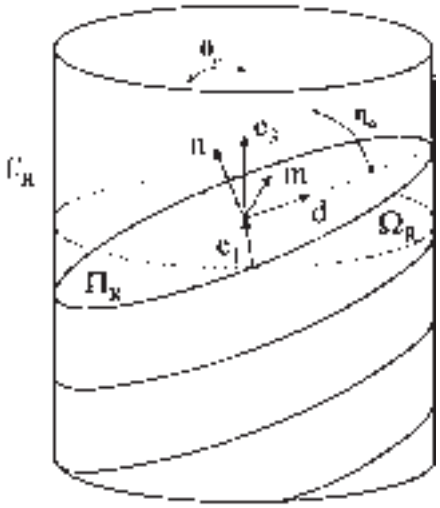

Figure 1. The geometry of single slip.

$$\begin{aligned} \mathbf{e}_3 &= \sin\theta_0\mathbf{d} + \cos\theta_0\mathbf{n} \\ &= \sin\theta_0(-\sin\eta_0\,\mathbf{n}\times\mathbf{m} + \cos\eta_0\mathbf{m}) + \cos\theta_0\mathbf{n}. \end{aligned} \tag{3.1}$$

It turns out that the vector $\mathbf{e}_1 := \mathbf{n}\times\mathbf{d}$ is parallel both to the slip plane and the cross-section Ω_R. A right-handed orthonormal basis can be defined in Ω_R by putting $\mathbf{e}_2 := \mathbf{e}_3\times\mathbf{e}_1$, and the following relationships hold:

$$\mathbf{e}_1 = \cos\eta_0\,\mathbf{n}\times\mathbf{m} + \sin\eta_0\mathbf{m} \tag{3.2}$$

$$\mathbf{e}_2 = \cos\theta_0(\sin\eta_0\,\mathbf{n}\times\mathbf{m} - \cos\eta_0\mathbf{m}) + \sin\theta_0\mathbf{n}. \tag{3.3}$$

The crystal is assumed to undergo a two-level shear from the reference configuration that is specified by giving:

(a) two scalars μ and γ,
(b) the two fixed and mutually orthogonal vectors $\mathbf{m}$, $\mathbf{n}$ introduced above, and a homogeneous deformation from $\mathcal{C}_R$ whose gradient is given by

$$\mathbf{F} = \mathbf{I} + \mu\mathbf{m}\otimes\mathbf{n}, \tag{3.4}$$

(c) the rotation $\mathbf{R}$ such that

$$\mathbf{RFe}_3 = \varepsilon \mathbf{e}_3, \tag{3.5}$$

with ε the elongation of a fiber in the direction $\mathbf{e}_3$,

$$\varepsilon := |\mathbf{RFe}_3| = |\mathbf{Fe}_3|\,, \tag{3.6}$$

and

(d) the tensor

$$\mathbf{G} = \mathbf{I} + \gamma\, \mathbf{m} \otimes \mathbf{n}. \tag{3.7}$$

From now on, we assume that μ is non-negative, so that the vector $\mathbf{m}$ points in the direction of shearing. The spatially constant tensor fields $\mathbf{RF}$ and $\mathbf{RG}$ represent, respectively, the macroscopic deformation and the deformation without slip for the underlying two-level shear.

We model Taylor's tensile experiments by assuming that total tensile loads $\mathbf{l}$ and $-\mathbf{l}$ are applied to the top and bottom faces Ω_R^+ and Ω_R^- in the form of dead loads:

$$\mathbf{l} = f\, area(\Omega_R)\mathbf{e}_3 = b\, area(\Omega)\frac{\mathbf{RFe}_3}{\varepsilon}, \tag{3.8}$$

where b and $area(\Omega)$ represent the applied force per unit area and the area in the deformed configuration, respectively, while f is the applied force per unit area in the reference configuration. In addition, we assume that the lateral surface of the crystal is traction free. If $\partial\mathcal{C} = \Omega^+ \cup \Omega^- \cup \mathcal{L}$ denotes the boundary of the crystal in the current configuration, our assumptions on the applied loads and the relation $b = \frac{f}{|(\mathbf{RF})^*\mathbf{e}_3|}$ (with $\mathbf{A}^* := (\det \mathbf{A})\mathbf{A}^{-T}$ denoting the adjugate of an invertible tensor $\mathbf{A}$) then yield on $\mathcal{L}$

$$\mathbf{T}(\mathbf{RF})^*\mathbf{e}_1 = \mathbf{T}(\mathbf{RF})^*\mathbf{e}_2 = 0 \tag{3.9}$$

and on $\Omega^+ \cup \Omega^-$

$$\frac{\mathbf{T}(\pm(\mathbf{RF})^*\mathbf{e}_3)}{|(\mathbf{RF})^*\mathbf{e}_3|} = \pm\frac{\mathbf{f}}{|(\mathbf{RF})^*\mathbf{e}_3|}\frac{\mathbf{RFe}_3}{\varepsilon}, \tag{3.10}$$

where $\mathbf{T}$ is the Cauchy stress and the "$+$" and "$-$" signs are taken on Ω^+ and Ω^-, respectively**.** It is easy to check that if we take for $\mathbf{T}$ the constant tensor field

$$\mathbf{T} = \frac{\mathbf{f}}{\varepsilon}\mathbf{RFe}_3 \otimes \mathbf{RFe}_3 = \varepsilon \mathbf{f}\mathbf{e}_3 \otimes \mathbf{e}_3, \tag{3.11}$$

then $\mathbf{T}$ satisfies (3.9) and (3.10) as well as the balance of forces and moments. By (3.1) and (3.4), the elongation ε defined in (3.5) can be evaluated explicitly:

$$\varepsilon = (1 + 2\mu \sin\theta_0 \cos\theta_0 \cos\eta_0 + \mu^2 \cos^2\theta_0)^{\frac{1}{2}}, \tag{3.12}$$

from which the scalar $\mathbf{T}\frac{(\mathbf{RF})^*\mathbf{n}}{|(\mathbf{RF})^*\mathbf{n}|} \cdot \frac{(\mathbf{RF})\mathbf{m}}{|(\mathbf{RF})\mathbf{m}|}$, the shear component of the Cauchy stress on the slip plane resolved in the direction of slip, is easily calculated:

$$\begin{aligned} \mathbf{T}\frac{(\mathbf{RF})^*\mathbf{n}}{|(\mathbf{RF})^*\mathbf{n}|} \cdot \frac{(\mathbf{RF})\mathbf{m}}{|(\mathbf{RF})\mathbf{m}|} &= \mathbf{TRn} \cdot \mathbf{Rm} \\ &= f\cos\theta_0 \frac{\mu + \tan\theta_0 \cos\eta_0}{(1 + \tan^2\theta_0 \sin\eta_0^2 + (\mu + \tan\theta_0 \cos\eta_0)^2)^{\frac{1}{2}}} \\ &= : \hat{\tau}_f(\mu). \end{aligned} \tag{3.13}$$

This expression agrees with the one obtained by Taylor ([1], p.212, (6)). The function $\hat{\tau}_f$ depends only on the amount of the load and on the orientation of the crystal in the loading device, and we call $\hat{\tau}_f$ the *load–orientation function* corresponding to f. The graph of $\hat{\tau}_f$ will be called the *load–orientation curve* corresponding to f.

4. ENERGETICS AND METASTABLE EQUILIBRIUM

For a body undergoing a two-level shear with f prescribed as in Section 3, the Gibbs free energy per unit volume can be obtained by subtracting from the Helmholtz free energy in (2.14) the work done per unit volume by the tractions, i.e.,

$$\mathcal{E}(\mu, \gamma; f) := \Psi(\mu, \gamma) - w(\mu; f), \tag{4.1}$$

where, by virtue of the boundary conditions for Taylor's soft device,

$$w(\mu; f) = \frac{1}{\ell_R \, area\Omega_R} \left(\int_{\Omega_R^+} \mathbf{S}\mathbf{e}_3 \cdot \mathbf{u} dA - \int_{\Omega_R^-} \mathbf{S}\mathbf{e}_3 \cdot \mathbf{u} dA \right), \tag{4.2}$$

and where $\mathbf{S}$ is the Piola–Kirchhoff stress tensor. Here, the dependence of $\mathbf{S}$ on f is determined by the formula (3.11) and by the formula $\mathbf{S} = \mathbf{T}(\mathbf{RF})^*$, and $\mathbf{u}$ is a displacement field satisfying $grad\mathbf{u} = \mathbf{RF} - \mathbf{I}$. By virtue of (3.4), (3.6), (3.11), and (3.13), after simple calculations, relation (4.2) yields

$$w(\mu; f) = \int_0^\mu \hat{\tau}_f(\zeta) d\zeta. \tag{4.3}$$

We wish to obtain two-level shears for prescribed f that are local minimizers of the Gibbs free energy function $(\mu,\gamma) \mapsto \mathcal{E}(\mu,\gamma;f) = \Psi(\mu,\gamma) - w(\mu;f)$. A pair (μ,γ) is a local minimizer for $\mathcal{E}$ only if the partial derivatives of $\mathcal{E}$ with respect to μ and with respect to γ both vanish, i.e., only if the pair (μ,γ) is a stationary point for $\mathcal{E}$:

$$\mathfrak{h}(\mu-\gamma)\psi_1'\left(\frac{1}{p}\int_0^{\mu-\gamma}\mathfrak{h}(r)dr\right) - \hat{\tau}_f(\mu) = 0 \tag{4.4}$$

$$\varphi'(\gamma) - \mathfrak{h}(\mu-\gamma)\psi_1'\left(\frac{1}{p}\int_0^{\mu-\gamma}\mathfrak{h}(r)dr\right) = 0. \tag{4.5}$$

(Here, the prime $'$ denotes differentiation with respect to γ or with respect to the argument of ψ_1.) From the stationary points, local minimizers (μ,γ) for $\mathcal{E}$ for a given f are obtained by imposing the condition that the Hessian of the Gibbs free energy be positive definite. It is easy to show that positive definiteness of the Hessian is equivalent to the positivity of the determinant of the Hessian, i.e.,

$$\varphi''(\gamma)\frac{\partial^2\Psi}{\partial\mu^2}(\mu,\gamma) - \frac{d}{d\mu}\hat{\tau}_f(\mu)\left(\varphi''(\gamma) + \frac{\partial^2\Psi}{\partial\mu^2}(\mu,\gamma)\right) > 0. \tag{4.6}$$

If for a given f and stationary point (μ,γ) for $\mathcal{E}$ we define

$$\tau := \varphi'(\gamma), \tag{4.7}$$

then equations (3.13), (4.4), and (4.5) tell us that τ is the resolved shear stress. From now on we call (μ,τ) a *stationary point* corresponding to $f \geq 0$ if the pair $(\mu,(\varphi')^{-1}(\tau))$ is a stationary point for $\mathcal{E}$. By (3.13), (4.4), (4.5), (4.7), and our earlier assumption $\mu \geq 0$, all of the stationary points lie in the first quadrant of the $\mu-\tau$ plane.

For each number $f \geq 0$, a stationary point (μ,τ) is called *metastable* if the inequality (4.6) holds with $\gamma = (\varphi')^{-1}(\tau)$. When the relation (4.6) holds with "$>$" replaced by "$=$", then the number f is called a *threshold load*, and the (non-metastable) stationary point (μ,τ) is called a *threshold point*. We note from (4.6) that the collection of threshold points and loads is determined by the functions φ, ψ_1, and $\mathfrak{h}$ in the formula (2.14) for the Helmholtz free energy Ψ and by the geometry of the crystal through the formula (3.13) for the load–orientation function $\hat{\tau}_f$. The assumptions (i) and (ii) made in Section 4.1 of reference [10] here will be made on the functions φ and $s \mapsto \psi_1(\frac{s}{p})$. In addition, we assume that the function $\mathfrak{h}$ is continuously differentiable.

In contrast to the dependence of threshold loads and threshold points on the functions φ, ψ_1, and $\mathfrak{h}$ in (2.14) as well as on the function $\hat{\tau}_f$ in relation (3.13), the parametric curve defined through the relations

$$\mu = \bar{\mu}(s) := s + (\varphi')^{-1}\left(\mathfrak{h}(s)\psi_1'\left(\frac{1}{p}\int_0^s\mathfrak{h}(r)dr\right)\right) \tag{4.8}$$

$$\tau \quad = \quad \bar{\tau}(s) := \mathfrak{h}(s)\psi_1' \left(\frac{1}{p} \int_0^s \mathfrak{h}(r) dr \right) \tag{4.9}$$

depends only upon φ, ψ_1, and $\mathfrak{h}$. If we allow s to be any non-negative number, then this curve traces out all of the stationary points (μ, τ) for $f \geq 0$ as well as other points in the fourth and possibly in the third quadrants in the $\mu - \tau$ plane. We call the curve described by (4.8) and (4.9) with $s \geq 0$ the *constitutive curve* for the crystal for the class of two-level shears under consideration.

Equations (4.4), (4.5), (4.8), and (4.9) ensure that the stationary points (μ, τ) for a given f form the intersection of the constitutive curve and the load orientation curve and provide, in conjunction with (3.13), a formula for the applied force per unit reference area f as a function of the shear due to slip s:

$$f = \bar{f}(s) := \frac{\bar{\tau}(s)}{\hat{\tau}_1(\bar{\mu}(s))} = \frac{\bar{\tau}(s)}{\hat{\tau}_1\left(s + (\varphi')^{-1}(\bar{\tau}(s))\right)}. \tag{4.10}$$

Differentiation of equation (2.14) twice with respect to μ and differentiation of equations (4.8), and (4.9) with respect to s, together with the positivity of φ'', yield an equivalent form of the metastability inequality (4.6):

$$\frac{d}{ds}\bar{\tau}(s) > \frac{d}{d\mu}\hat{\tau}_{f(s)}\,(\mu)\,|_{\mu=\bar{\mu}(s)}\;\frac{d}{ds}\bar{\mu}(s). \tag{4.11}$$

When the inequality (4.11) holds, the non-negative number s will be called a *metastable slip*; when equality (in place of "$>$") holds in (4.11), s will be called a *threshold slip*. Henceforth, in referring to $s = \mu - \gamma$ we will use the shorter term *slip* in place of *shear due to slip*. For threshold slips we may write

$$\frac{\frac{d}{ds}\bar{\tau}(s)}{\frac{d}{ds}\bar{\mu}(s)} = \frac{d}{d\mu}\hat{\tau}_{\bar{f}(s)}\,(\mu)|_{\mu=\bar{\mu}(s)} \tag{4.12}$$

which expresses a tangency condition: threshold slips correspond to points $(\bar{\mu}(s), \bar{\tau}(s))$ in the $\mu - \tau$ plane at which the constitutive curve (4.8), (4.9) and the load–orientation curve (3.13) for the load $\bar{f}(s)$ are tangent. The terminology introduced above (4.8) and (4.9) along with the equivalence of (4.6) and (4.12) justify our using the term *threshold points* for these points of tangency.

Our aim in the remainder of this section is to provide a general analysis of the form of the constitutive curve (4.8), (4.9), particularly in relation to threshold and other distinguished points to be introduced below. (In this analysis, we prefer using the one symbol $'$ to denote differentiation of a function, rather than using a variety of symbols $\frac{d}{ds}$, $\frac{d}{d\mu}$, etc.) To begin this analysis, we record formulas obtained by differentiating relations (4.8) and (4.9)**:**

$$\bar{\mu}'(s) = \frac{\bar{\tau}'(s) + \varphi''\left((\varphi')^{-1}(\bar{\tau}(s))\right)}{\varphi''\left((\varphi')^{-1}(\bar{\tau}(s))\right)}, \tag{4.13}$$

which shows that $\bar{\mu}'(s)$ and $\bar{\tau}'(s)$ do not both vanish and justifies placing $\frac{d}{ds}\bar{\mu}(s)$ in the denominator of the left-hand side of equation (4.12),

$$\frac{\bar{\tau}'(s)}{\bar{\mu}'(s)} = \frac{\bar{\tau}'(s)\boldsymbol{\varphi}''\left((\boldsymbol{\varphi}')^{-1}(\bar{\tau}(s))\right)}{\bar{\tau}'(s) + \boldsymbol{\varphi}''\left((\boldsymbol{\varphi}')^{-1}(\bar{\tau}(s))\right)}, \tag{4.14}$$

and

$$\bar{\tau}'(s) = \mathfrak{h}'(s)\psi_1'\left(\frac{1}{p}\int_0^s \mathfrak{h}(r)dr\right) + \frac{\mathfrak{h}^2(s)}{p}\psi_1''\left(\frac{1}{p}\int_0^s \mathfrak{h}(r)dr\right). \tag{4.15}$$

In order to describe the constitutive curve and, in particular, the metastable points, we single out *fundamental intervals* of slip $I_j := [s^o_{2j}, \mu^o_{2j+1}]$, $j = 0, 1, 2, \cdots$, with s^o_{2j} and μ^o_{2j+1} distinguished values of slip to be defined presently, and we call $\{(\bar{\mu}(s), \bar{\tau}(s)) \mid s \in I_j\}$ the $j+1^{st}$ *fundamental branch* of the constitutive curve. For each $j = 0, 1, 2, \cdots$, both the left endpoint $s^o_{2j} := \mu^o_{2j}$ and the right endpoint μ^o_{2j+1} of I_j are obtained from the collection $\{\mu^o_k \mid k = 0, 1, 2, \cdots\}$ of slips defined as the solutions of the equation

$$\int_0^{\mu^o_k} \mathfrak{h}(r)dr = \frac{kp}{2}. \tag{4.16}$$

When the function $\mathfrak{h}$ is strictly increasing, these slips satisfy $\mu^o_k < \mu^o_{k+1}$ and $\mu^o_{k+2} - \mu^o_{k+1} < \mu^o_{k+1} - \mu^o_k$ for all $k = 0, 1, 2, \cdots$. We define also for each $j = 0, 1, 2, \cdots$ a slip $s^q_{2j} \in (s^o_{2j}, \mu^o_{2j+1})$ as the unique solution of the equation

$$\int_{s^o_{2j}}^{s^q_{2j}} \mathfrak{h}(r)dr = \frac{p}{4}, \tag{4.17}$$

and we note that, by (4.9), (4.15), (4.16), and the assumption (ii) on ψ_1

$$\bar{\tau}(s^o_{2j}) = \bar{\tau}(\mu^o_{2j+1}) = 0, \quad \bar{\tau}'(s^q_{2j}) = \mathfrak{h}'(s^q_{2j})\psi_1'(\tfrac{1}{4}) \geq 0. \tag{4.18}$$

Moreover, both terms on the right-hand side of (4.15) are non-negative for all $s \in [s^o_{2j}, s^q_{2j}] \subset I$, $\bar{\tau}'(s^o_{2j}) = \frac{\mathfrak{h}^2(s^o_{2j})}{p}\psi_1''(0) > 0$, and $\bar{\tau}'(\mu^o_{2j+1}) = \frac{\mathfrak{h}^2(\mu^o_{2j+1})}{p}\psi_1''(\frac{1}{2}) < 0$. Therefore, there is at least one number $s \in [s^q_{2j}, \mu^o_{2j+1}) \subset I_j$ such that $\bar{\tau}'(s) = 0$, and we denote by s^m_{2j} the smallest one. Finally, by (4.14), (4.18), (4.9), and (4.10) we have:

$$\frac{\bar{\tau}'(s^o_{2j})}{\bar{\mu}'(s^o_{2j})} - \bar{f}(s^o_{2j})\hat{\tau}_1'(\bar{\mu}(s^o_{2j})) > 0 \tag{4.19}$$

$$\frac{\bar{\tau}'(s^m_{2j})}{\bar{\mu}'(s^m_{2j})} - \bar{f}(s^m_{2j})\hat{\tau}_1'(\bar{\mu}(s^m_{2j})) < 0. \tag{4.20}$$

Consequently, there is at least one number $s \in (s^o_{2j}, s^m_{2j}) \subset I_j$ such that the tangency condition (4.12) holds, and we denote by s^t_{2j} the smallest one.

In Section 5 we shall employ as $p \to 0$ and $j \to \infty$, with the product jp bounded, the following order of magnitude relations among the distinguished slips s^o_{2j}, s^q_{2j}, s^t_{2j}, and s^m_{2j} just introduced:

$$\mu^o_{2j+1} = s^o_{2j} + O(p) \tag{4.21}$$

$$s^q_{2j} = s^o_{2j} + O(p) \tag{4.22}$$

$$s^t_{2j} = s^q_{2j} + O(p^2) \tag{4.23}$$

$$s^m_{2j} = s^q_{2j} + O(p^2). \tag{4.24}$$

Moreover, relation (4.23) holds when s^t_{2j} is replaced by an arbitrary number $s \in (s^o_{2j}, s^m_{2j})$ at which the tangency condition (4.12) holds, and relation (4.24) holds when s^m_{2j} is replaced by an arbitrary number $s \in [s^q_{2j}, \mu^o_{2j+1}]$ such that $\bar{\tau}'(s) = 0$. The proofs of (4.21)–(4.24) are provided in the Appendix; the proofs of (4.23) and (4.24) require the additional assumptions

$$\text{(iii)} \qquad \psi_1'''(\tfrac{1}{4}) < 0$$

and (A.20) in the Appendix.

It is worth noting that the constitutive assumptions (i), (ii), and (iii) on φ and ψ_1 do not rule out the possibility of having more than one threshold point, more than one local high point or low point, or more than one point of vertical tangency on each fundamental branch. However, the order of magnitude relations (4.23), (4.24) ensure that, for each $s_0 > 0$, when p is sufficiently small and with $j = \frac{s_0}{p}$, the threshold points and the points $(\bar{\mu}(s), \bar{\tau}(s))$ at which $\bar{\tau}'(s) = 0$ are clustered together in the $(j+1)$th fundamental branch, close to the "quarter point" $(\bar{\mu}(s^q_{2j}), \bar{\tau}(s^q_{2j}))$, with s^q_{2j} the unique solution of equation (4.17). Qualitative features of a typical fundamental branch of the constitutive curve are shown in Figure 2. At the end of Section 7 we provide conditions on the constitutive functions φ and $\mathfrak{h}$ and on the load–orientation function $\hat{\tau}_1$ defined through (3.13) ensuring that each load–orientation curve crosses every fundamental branch of the constitutive curve from some point on.

In spite of the rather complicated shape of the constitutive curve, an intrinsic energetic relation can be established.

Remark 1. For every pair of points $A := (\bar{\mu}(s^a), \bar{\tau}(s^a))$ and $B := (\bar{\mu}(s^b), \bar{\tau}(s^b))$ on the constitutive curve, with $0 \le s^a \le s^b$, the difference in free energy is given by

$$\begin{aligned} \Psi_B - \Psi_A &= \int_{\Gamma^B_A} \left(\frac{\partial \Psi}{\partial \mu} d\mu + \frac{\partial \Psi}{\partial \gamma} \frac{d\gamma}{d\tau} d\tau \right) \\ &= \int_{\Gamma^B_A} \varphi'(\gamma) d\mu = \int_{\Gamma^B_A} \varphi'((\varphi')^{-1}(\tau)) d\mu \end{aligned}$$

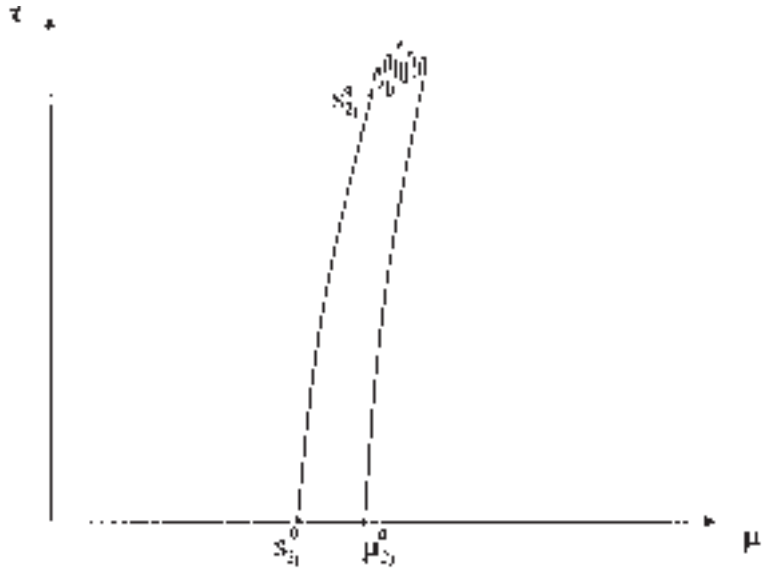

Figure 2. The jth fundamental branch of the constitutive locus with points labeled by values of the slip s.

$$= \int_{\Gamma_A^B} \tau d\mu, \tag{4.25}$$

with $\Gamma_A^B := \{(\bar{\mu}(s), \bar{\tau}(s)) \mid s \in [s^a, s^b]\}$ the segment of the constitutive curve connecting A and B. Because the last term of this relation is the work done by the resolved shear stress as the point $(\bar{\mu}(s), \bar{\tau}(s))$ smoothly follows Γ_A^B, the dissipation inequality

$$\Psi_B - \Psi_A \leq \int_{\Gamma_A^B} \tau d\mu \tag{4.26}$$

is satisfied with equality.

The relation (4.25) follows from the fact that every point (μ, τ) on the constitutive curve corresponds to a stationary point $(\mu, \gamma) = (\mu, (\varphi')^{-1}(\tau))$ for the total energy $\mathcal{E}$, so that $\frac{\partial \mathcal{E}}{\partial \mu} = \frac{\partial \Psi}{\partial \mu} - \hat{\tau}_f(\mu) = 0$ and $\frac{\partial \mathcal{E}}{\partial \gamma} = \frac{\partial \Psi}{\partial \gamma} = 0$, as in (4.1) and (4.5), with Ψ given by (2.14). According to this remark, smooth evolution following the constitutive curve occurs without dissipation. In the next section we identify the source of dissipation during loading processes of the crystal.

5. LOADING AND THE PORTEVIN–LE CHATELIER EFFECT

In order to explain in this section the picture of loading of a crystal that emerges from the considerations in Section 4, we restrict our attention initially to the case where every fundamental branch of the constitutive curve is a simple curve that has exacly one slip $s_{2j}^m \in$

$(s^o_{2j}, \mu^o_{2j+1}) \subset I_j$ at which $\bar{\tau}'(s^m_{2j}) = 0$ and at most one slip $\tilde{s}^m_{2j} \in (s^o_{2j}, \mu^o_{2j+1}) \subset I_j$ satisfying $\bar{\mu}'(\tilde{s}^m_{2j}) = 0$. In addition, we assume that for each load–orientation curve and for each fundamental branch of the constitutive curve, either the two loci cross exactly twice or they do not cross (the latter includes both the case where the loci are disjoint and the case where the loci are tangent). This special case for the constitutive curve is depicted in Figure 3. We note for future reference that by relation (4.13) the slips s^m_{2j} and $\tilde{s}^m_{2j}$ satisfy $s^m_{2j} < \tilde{s}^m_{2j}$.

Suppose now that the crystal initially is deformed in the trivial two-level shear $\mu = \gamma = 0$ under zero applied load and, subsequently, is subjected to a monotonically increasing applied load. We assume that the crystal responds first by attaining two-level shears with slips $s = \mu - \gamma$ in the first fundamental interval $I_0 = [s^o_0, \mu^o_1] = [0, \mu^o_1]$. As the applied load is increased from 0 to the smallest threshold load $\bar{f}(s^t_0)$, it is consistent with metastability to expect that the crystal will deform in such a way that the macroshear and the resolved shear stress will follow the metastable points $\{(\bar{\mu}(s), \bar{\tau}(s)) \mid 0 \le s < s^t_0\}$. According to Remark 1, for each $s^a, s^b \in [0, s^t_0)$, with $s^a < s^b$, we may write

$$\Psi\left(\bar{\mu}(s^b), (\boldsymbol{\varphi}')^{-1}(\bar{\tau}(s^b))\right) - \Psi\left(\bar{\mu}(s^a), (\boldsymbol{\varphi}')^{-1}(\bar{\tau}(s^a))\right) = \int_{s^a}^{s^b} \bar{\tau}(s)\bar{\mu}'(s)ds, \tag{5.1}$$

so that *the shearing associated with the increase in f from 0 to $\bar{f}(s^t_0)$ occurs without dissipation*.

The threshold point $A := (\bar{\mu}(s^t_0), \bar{\tau}(s^t_0))$ in Figure 4, reached when f assumes the threshold value $\bar{f}(s^t_0)$, is *not* metastable. It is consistent with this lack of metastability to expect that the crystal under the load $\bar{f}(s^t_0)$ will deform so that the macroshear and the resolved shear stress will achieve a different point B on the intersection of the constitutive curve and the load–orientation curve $\tau = \hat{\tau}_{\bar{f}(s^t_0)}(\mu)$ through the threshold point A, a point B that is metastable and at which the crystal has a lower Gibbs free energy than it does at A. In order to study this possibility, we introduce the set

$$\mathcal{I}_1 := \left\{(\bar{\mu}(s), \bar{\tau}(s)) \mid s \in I_1 \text{ and } \bar{\tau}(s) = \hat{\tau}_{\bar{f}(s^t_0)}(\bar{\mu}(s))\right\} \tag{5.2}$$

of points of intersection of the load–orientation curve for $\bar{f}(s^t_0)$ with the next fundamental branch $\{(\bar{\mu}(s), \bar{\tau}(s)) \mid s \in I_1\}$ of the constitutive curve. We recall from Section 4 that the interval I_1 determines the second fundamental branch of the constitutive curve and is given by $I_1 = [s^o_2, \mu^o_3]$. Our assumptions in the first paragraph of this section yield two possibilities: (1) $\mathcal{I}_1$ contains no crossing points of the load–orientation curve and the second fundamental branch or (2) $\mathcal{I}_1$ contains exactly two crossing points. In the first case (1), the set $\mathcal{I}_1$ consists of at most one point, necessarily a threshold point and, therefore, not metastable. We interpret this case to mean that the crystal under the threshold load $\bar{f}(s^t_0)$ will not deform from the threshold slip $s^t_0 \in I_0$ by means of a two-level shear with slip $s = \mu - \gamma \in I_1$.

We procede now to the analysis of the second case (2), and we denote by s^c_2 the smaller of the two slips in the interval $(s^o_2, \mu^o_3) \subset I_1$ for which $B := (\bar{\mu}(s^c_2), \bar{\tau}(s^c_2)) \in \mathcal{I}_1$ is a crossing point, as depicted in Figure 3. Our goal is to show that B is metastable and corresponds to a lower Gibbs free energy for the crystal than does the threshold point $A = (\bar{\mu}(s^t_0), \bar{\tau}(s^t_0))$. The fact that the load–orientation curve crosses the fundamental branch $\mathcal{I}_1$ at the slip $s^c_2 > s^t_0$

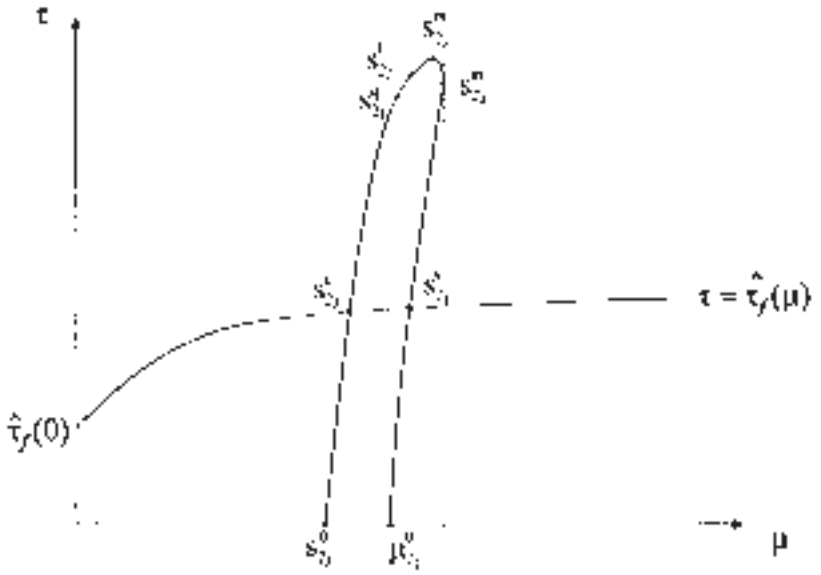

Figure 3. A load–orientation curve and the jth fundamental branch for the special case, with points labeled by values of the slip s.

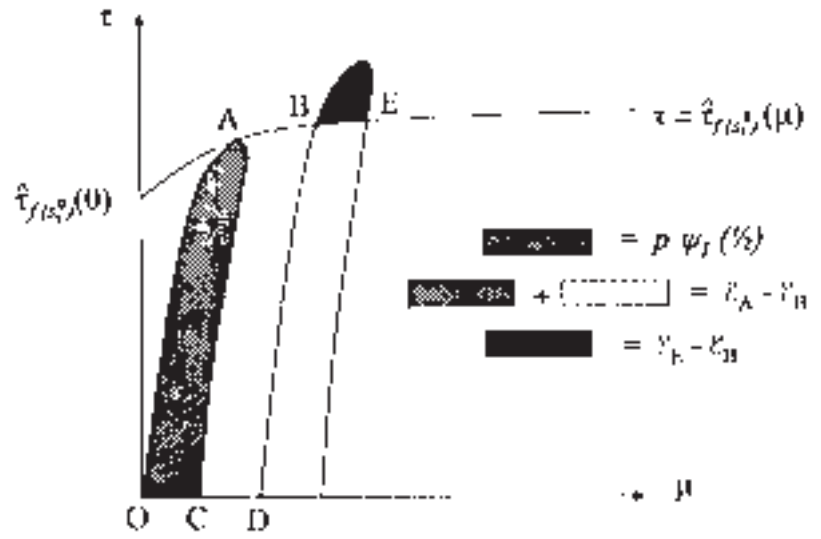

Figure 4. Energy changes along a load–orientation curve.

implies that relation (4.11) is satisfied with $s = s_2^c$ and, therefore, that B is a metastable point. In order to compare the Gibbs free energies at A and at B, we let $C := (\mu_1^o, 0)$ and $D := (s_2^o, 0)$ denote, respectively, the points at the end of the first fundamental branch $\mathcal{I}_0$ and at the beginning of the second fundamental branch $\mathcal{I}_1$ (see Figure 4), and we write

$$\Psi_B - \Psi_A = (\Psi_B - \Psi_D) + (\Psi_D - \Psi_C) + (\Psi_C - \Psi_A) \tag{5.3}$$

as well as

$$\int_{\Gamma_D^B \cup \bar{\Gamma}_C^D \cup \Gamma_A^C} \tau d\mu = \int_{\Gamma_D^B} \tau d\mu + \int_{\bar{\Gamma}_C^D} \tau d\mu + \int_{\Gamma_A^C} \tau d\mu,$$

where

$$\begin{aligned} \Gamma_D^B &: = \{(\bar{\mu}(s), \bar{\tau}(s)) \mid s \in [s_2^o, s_2^c]\} \\ \bar{\Gamma}_C^D &: = \{(\mu, 0) \mid \mu \in [\mu_1^o, s_2^o]\} \\ \Gamma_A^C &: = \left\{(\bar{\mu}(s), \bar{\tau}(s)) \mid s \in [s_0^t, \mu_1^o]\right\}. \end{aligned} \tag{5.4}$$

Relations (2.14), (4.16), (4.1), and the periodicity of ψ_1 imply that

$$\Psi_D - \Psi_C = -p\psi_1(\tfrac{1}{2}), \quad \mathcal{E}_C - \mathcal{E}_O = \Psi_C - \Psi_O = p\psi_1(\tfrac{1}{2}) \tag{5.5}$$

where O denotes the origin in the $\mu - \tau$ plane**.** If we note that $\tau = 0$ at each point of $\bar{\Gamma}_C^D$ and use Remark 1 to evaluate $\Psi_B - \Psi_D$ and $\Psi_C - \Psi_A$, relations (5.3)–(5.5) yield

$$\begin{aligned} \Psi_B - \Psi_A &= \int_{\Gamma_D^B \cup \bar{\Gamma}_C^D \cup \Gamma_A^C} \tau d\mu - p\psi_1(\tfrac{1}{2}) \\ &= \int_{\Gamma_D^B \cup \bar{\Gamma}_C^D \cup \Gamma_A^C \cup \mathcal{L}_B^A} \tau d\mu + \int_{\mathcal{L}_A^B} \tau d\mu - p\psi_1(\tfrac{1}{2}) \end{aligned} \tag{5.6}$$

where $\mathcal{L}_A^B := \left\{(\bar{\mu}(s), \hat{\tau}_{\bar{f}(s_0^t)}(\bar{\mu}(s)) \mid s \in [s_0^t, s_2^c]\right\}$ is the segment of the load–orientation curve that connects the threshold point $A = (\bar{\mu}(s_0^t), \bar{\tau}(s_0^t))$ to the metastable crossing point $B = (\bar{\mu}(s_2^c), \bar{\tau}(s_2^c))$, and $\mathcal{L}_B^A$ is its reversal. Green's Theorem may now be applied to transform the line integral along the simple, closed, positively-oriented curve $\Gamma_D^B \cup \bar{\Gamma}_C^D \cup \Gamma_A^C \cup \mathcal{L}_B^A$ to obtain the formula

$$\Psi_B - \Psi_A = -area(\mathcal{A}_{ACDBA}) - p\psi_1(\tfrac{1}{2}) + \int_{\bar{\mu}(s_0^t)}^{\bar{\mu}(s_2^c)} \hat{\tau}_{\bar{f}(s_0^t)}(\mu) d\mu \tag{5.7}$$

with $\mathcal{A}_{ACDBA}$ denoting the interior of $\Gamma_D^B \cup \bar{\Gamma}_C^D \cup \Gamma_A^C \cup \mathcal{L}_B^A$. From (4.1), (4.3), and (5.7) it follows that

$$\mathcal{E}_B - \mathcal{E}_A = -area(\mathcal{A}_{ACDBA}) - p\psi_1(\tfrac{1}{2}) < 0, \tag{5.8}$$

so that the Gibbs free energy at the threshold point A is greater than the Gibbs free energy at the metastable crossing point B.

In summary, case (2) is characterized by the fact that the load orientation curve for the threshold load $\bar{f}(s_0^t)$ connects the threshold point A with energy $\mathcal{E}_A$ to the stable crossing point B with energy $\mathcal{E}_B < \mathcal{E}_A$. We interpret this situation to mean that it is energetically favorable for the crystal under the fixed load $\bar{f}(s_0^t)$ to deform from the two-level shear with $\mu = \bar{\mu}(s_0^t), \gamma = (\varphi')^{-1}(\bar{\tau}(s_0^t))$ to the two-level shear with $\mu = \bar{\mu}(s_2^c), \gamma = (\varphi')^{-1}(\bar{\tau}(s_2^c))$. We describe the mechanism for this deformation as a *material instability at the mesolevel*, and we note that the slip s jumps in this deformation from the threshold value $s_0^t \in I_0$ to the value $s_2^c \in I_1$. There are corresponding jumps in the macroshear μ, in the shear without slip γ, and in the free energy Ψ, and the relation (5.7) ensures that the change in free energy in this jump is less than the work done by the applied threshold load. Thus, the dissipation inequality

$$\Psi_B - \Psi_A \leq \int_{\bar{\mu}(s_0^t)}^{\bar{\mu}(s_2^c)} \hat{\tau}_{\bar{f}(s_0^t)}(\mu) d\mu \tag{5.9}$$

is satisfied with strict inequality, i.e., *the jump in slip $s_2^c - s_0^t$ is dissipative.*

In order to complete the analysis of case (2), we consider the second crossing point on the second fundamental branch: $E := (\bar{\mu}(\tilde{s}_2^c), \bar{\tau}(\tilde{s}_2^c))$ where $s_2^c < s_2^m < \tilde{s}_2^c \in I_1$. From Figure 4, Remark 1, and Green's Theorem (with notation analogous to that used in the previous argument), we conclude that

$$\begin{aligned} \mathcal{E}_E - \mathcal{E}_B &= \Psi_E - \Psi_B - \int_{\mathcal{L}_B^E} \tau d\mu \\ &= \int_{\Gamma_B^E} \tau d\mu + \int_{\mathcal{L}_E^B} \tau d\mu = \int_{\Gamma_B^E \cup \mathcal{L}_E^B} \tau d\mu \\ &= area(int(\Gamma_B^E \cup \mathcal{L}_E^B)) > 0. \end{aligned} \tag{5.10}$$

Between the two crossing points B and E in the fundamental branch $\mathcal{I}_1$, the point B corresponds to a lower Gibbs free energy for the crystal, so that, under the threshold load $\bar{f}(s_0^t)$, the dissipative jump in slip from s_0^t to s_2^c is energetically more favorable than that from s_0^t to $\tilde{s}_2^c$. Because s_2^c corresponds to a metastable crossing point that has lowest energy among the crossing points in that fundamental branch, we say that the slip s_2^c is *attainable* from s_0^t under the threshold load $\bar{f}(s_0^t)$, and, analogously, that the crossing point $B = (\bar{\mu}(s_2^c), \bar{\tau}(s_2^c))$ is *attainable* from the threshold point $A = (\bar{\mu}(s_0^t), \bar{\tau}(s_0^t))$ under that load.

If for each positive interger j we put

$$\mathcal{I}_j := \left\{ (\bar{\mu}(s), \bar{\tau}(s)) \mid s \in I_j \text{ and } \bar{\tau}(s) = \hat{\tau}_{\bar{f}(s_0^t)}(\bar{\mu}(s)) \right\}, \tag{5.11}$$

then the analysis given above for $\mathcal{I}_1$ applies to $\mathcal{I}_j$, and we obtain (still in case (2)) a distinguished slip $s^c_{2j} \in I_j$, attainable from s^t_0 under the threshold load $\bar{f}(s^t_0)$, as well as the corresponding point $(\bar{\mu}(s^c_{2j}), \bar{\tau}(s^c_{2j})) \in \mathcal{I}_j$ attainable from the threshold point $A = (\bar{\mu}(s^t_0), \bar{\tau}(s^t_0))$ under that load. Letting $j < k$ be positive integers and letting $\mathcal{E}_j$ and $\mathcal{E}_k$ be the energies at the corresponding attainable slips $s^c_{2j} \in I_j$ and $s^c_{2k} \in I_k$, we have by (5.8) with obvious modifications

$$\mathcal{E}_k - \mathcal{E}_j = (\mathcal{E}_k - \mathcal{E}_A) - (\mathcal{E}_j - \mathcal{E}_A) = -area(\mathcal{A}_{jk}), \tag{5.12}$$

where $\mathcal{A}_{jk}$ is the region in the $\mu - \tau$ plane bounded by the μ-axis, the load–orientation curve, and the segments $\left\{ (\bar{\mu}(s), \bar{\tau}(s)) \mid s \in [s^o_{2j}, s^c_{2j}] \right\}$ and $\left\{ (\bar{\mu}(s), \bar{\tau}(s)) \mid s \in [s^o_{2k}, s^c_{2k}] \right\}$ of the constitutive curve. Thus, *for a given threshold load, the Gibbs free energy at a larger attainable slip is less than the energy at a smaller attainable slip*.

The monotonically decreasing energy profile of successive attainable points for a given threshold load permits a crystal to undergo further dissipative shearing from a given attainable point for that load. Nevertheless, the passage from one attainable point $(\bar{\mu}(s^c_{2j}), \bar{\tau}(s^c_{2j})) \in \mathcal{I}_j$ to another $(\bar{\mu}(s^c_{2k}), \bar{\tau}(s^c_{2k})) \in \mathcal{I}_k$ for a given threshold load entails overcoming an energy barrier, analogous to that calculated in (5.10), between the two crossing points $(\bar{\mu}(s^c_{2j}), \bar{\tau}(s^c_{2j}))$ and $(\bar{\mu}(\tilde{s}^c_{2j}), \bar{\tau}(\tilde{s}^c_{2j}))$ in $\mathcal{I}_j$ (see Figure 3). Depending upon the availability of energy for the crystal in the loading device, this and successive energy barriers may provide a limitation on the attainable slips.

The present description of the initial response of the crystal depicts the crystal undergoing a shearing without dissipation from the origin $O = (0, 0)$ to the threshold point $A = (\bar{\mu}(s^t_0), \bar{\tau}(s^t_0))$ as the load increases from zero to the first threshold value $\bar{f}(s^t_0)$, followed by a shearing with dissipation from the threshold point $(\bar{\mu}(s^t_0), \bar{\tau}(s^t_0))$ to an attainable point $(\bar{\mu}(s^c_{2j}), \bar{\tau}(s^c_{2j}))$ under the threshold load $\bar{f}(s^t_0)$. The shearing without dissipation follows the constitutive curve, while the shearing with dissipation follows the load–orientation curve. If we replace in this description the initial point $(0, 0)$ by the attainable point $(\bar{\mu}(s^c_{2j}), \bar{\tau}(s^c_{2j}))$, the arguments above may be repeated. In particular, as the load increases from the first threshold value $\bar{f}(s^t_0)$ to the jth threshold value $\bar{f}(s^t_{2j})$, the crystal undergoes a shearing without dissipation that follows the jth fundamental branch of the constitutive curve from the attainable point $(\bar{\mu}(s^c_{2j}), \bar{\tau}(s^c_{2j}))$ to the threshold point $(\bar{\mu}(s^t_{2j}), \bar{\tau}(s^t_{2j}))$, followed by a shearing with dissipation in which the pair (μ, τ) jumps along the load–orientation curve corresponding to $\bar{f}(s^t_{2j})$ to a new attainable point $(\bar{\mu}(s^c_{2k}), \bar{\tau}(s^c_{2k}))$ with $k > j$.

Although the resolved shear stresses $\bar{\tau}(s^t_{2j})$ at threshold points do signal the occurrence of irreversible slip, we hesitate to assign to them commonly used terms such as "flow stress", "initial critical strength", and "critical resolved shear stress" [5, 15], because these terms are understood as constitutive properties of a crystal, independent of a particular loading device, whereas $\bar{\tau}(s^t_{2j})$ depends on both the crystal and the loading device. In Sections 6 and 7 we recover purely constitutive quantities that signal the occurrence of irreversible slip, at which point we adopt the commonly used terminology.

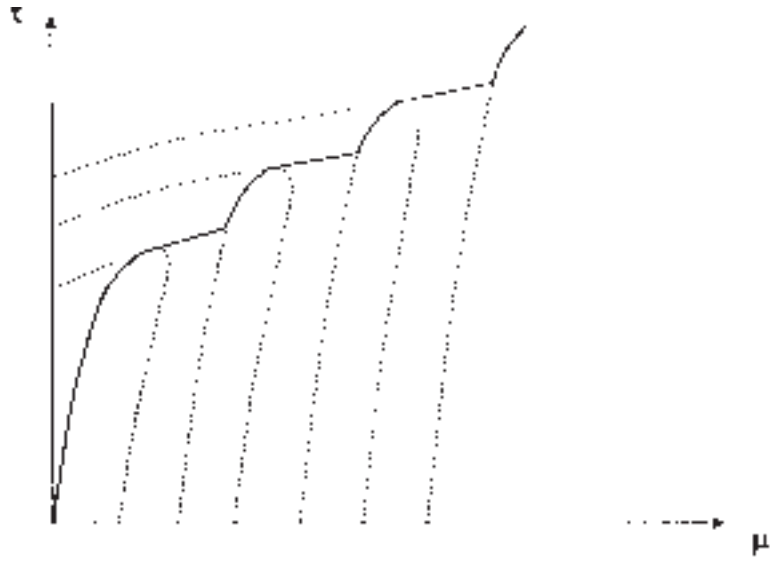

Figure 5. Staircase locus.

The alternating shearing without dissipation along fundamental branches of the constitutive curve and shearing with dissipation along threshold load–orientation curves produces a rising "staircase locus", as depicted in Figure 5. Qualitatively similar staircase loci are observed in experiments on single crystals in soft loading devices, and their appearance is called the Portevin–le Chatelier effect [16–18]. According to the theory given so far in this section, the experimental points on a given dissipative segment of the staircase locus must be attainable points for the given threshold load and, hence, must have a minimum separation on that segment. This minimum separation may vary from segment to segment. In contrast, the experimental points on each non-dissipative segment are permitted to be arbitrary metastable points on a fundamental branch of the constitutive locus and, hence, can be arbitrarily close together within the precision of the experiment. We note that a lower bound for the minimum separation $s_{2k}^{\exp} - s_{2j}^{\exp}$ of consecutive experimental values $s_{2k}^{\exp} > s_{2j}^{\exp}$ of slip for a given threshold load can be obtained from relation (10.4) in the Appendix:

$$\frac{p}{\mathfrak{h}((j+\frac{1}{2})p)} \leq s_{2k}^{\exp} - s_{2j}^{\exp}; \tag{5.13}$$

here, $s_{2j}^{\exp} := \mu_{2j}^{\exp} - (\varphi')^{-1}(\tau_{2j}^{\exp})$ and $s_{2k}^{\exp} := \mu_{2k}^{\exp} - (\varphi')^{-1}(\tau_{2k}^{\exp})$, with $(\mu_{2j}^{\exp}, \tau_{2j}^{\exp})$ and $(\mu_{2k}^{\exp}, \tau_{2k}^{\exp})$ consecutive experimental points for the given threshold load.

The present theoretical description of slip in single crystals also suggests that, for a given threshold load, the likelihood that the crystal undergoes further dissipative shearing from a specified attainable point will increase with the amount of time that the threshold load is applied, because a longer application of the load increases the probability that a given energy barrier can be crossed by means of thermal fluctuations, for example. Consequently, we

expect that slower loading programs would produce wider dissipative steps in the staircase locus than would rapid loading programs.

We close this section by indicating how the restrictions that were imposed in the first paragraph of this section on the constitutive curve and on load–orientation curves can be relaxed without altering our conclusions. Specifically, we can replace the initial restriction by the weaker assumption that the integral $\int_{\mathcal{C}} \tau d\mu$, with $\mathcal{C}$ a closed curve bounding either the region $int(\Gamma_B^E \cup \mathcal{L}_E^B)$ in (5.10) or the region $\mathcal{A}_{jk}$ in (5.12), is a finite sum of integrals around simple closed curves. The weaker assumption permits each set $\mathcal{I}_j$ to have more than two, but at most finitely many points. In particular, it may happen that the jumps in slip between a threshold point and a subsequent metastable point can occur within one and the same fundamental interval I_j. Therefore, the dissipative segments of the staircase locus can now join points within a single fundamental branch of the constitutive curve. The analysis that established (5.10) together with the order of magnitude relations (4.23), (4.24) can be employed to show that the energy change from a given point in $\mathcal{I}_j$ to a neighboring point in $\mathcal{I}_j$ with larger slip is of order $O(p^2)$ or is of order $O(p)$ and positive. Thus, dissipative jumps between points in one and the same fundamental branch either entail comparatively small energy changes, because p is of the order 10^{-4} for many crystals, or are energetically unfavorable. On the other hand, the analysis underlying (5.12) together with (4.23), (4.24) shows that the energy change in a jump from a threshold point in one principal branch to a metastable point in a subsequent branch is negative and of the order $O(p)$, i.e., such jumps are energetically favorable and entail non-negligible energy changes.

6. THE INITIAL CRITICAL RESOLVED SHEAR STRESS

The constitutive curve (4.8), (4.9) is completely determined by the lattice distortion energy density φ, the slip energy density ψ_1, and the function $\mathfrak{h}$. In this section, we provide a physical interpretation for the constitutive quantity $\max \psi_1'$ that is based on the formula

$$\max \psi_1' = \lim_{p \to 0} \bar{\tau}(s_0^t(p)), \tag{6.1}$$

to be verified below. Here, $\bar{\tau}$ is the constitutive function defined in (4.9), and $s_0^t(p)$ is the smallest threshold slip for the given crystal in the Taylor soft device, introduced below (4.20) (we indicate here for the first time the explicit dependence of this slip on the parameter p). We note that, for each positive number p, the threshold shear stress $\bar{\tau}(s_0^t(p))$ is the value of the resolved shear stress at a point in the μ-τ plane where the constitutive curve and the load–orientation curve are tangent and, among such points, it is the point at which the slip s has its smallest value. It is then apparent that the threshold shear stress $\bar{\tau}(s_0^t(p))$ depends not only upon the material composing the crystal but also upon the particular device that gives rise to the load–orientation curves. Therefore, relation (6.1) tells us that the device- and material-dependent quantity $\bar{\tau}(s_0^t(p))$ tends to the number $\max \psi_1'$ that depends upon the material but not upon the loading device. In other words, $\bar{\tau}(s_0^t(p))$ is a device-dependent approximation to the constitutive quantity $\max \psi_1'$ that tends to $\max \psi_1'$ as p tends to zero.

The positive number $\tau_c := \max \psi_1'$ from now on will be called the *initial critical resolved shear stress* or the *initial critical strength* of the crystal (for the slip system specified at the

beginning of Section 3). The origin of these terms is discussed in [5], pp.10–11. According to the present theory, for each p, only non-dissipative shearing may occur for values of the resolved shear stress below $\bar{\tau}(s_0^t(p))$, so that the initial critical resolved shear stress τ_c is the limit as $p \to 0$ of the minimum shear stress at which dissipative shearing may occur. In interpreting the condition $p \to 0$, it is useful to recall from Section 2 that p is the reciprocal of $\hat{d}(0)$, the relative separation of active slip bands when $s = 0$; consequently, the condition $p \to 0$ is equivalent to $\hat{d}(0) \to \infty$. Relations (2.2)–(2.4) tell us that the last limit corresponds to having the separation of active slip bands in the reference configuration become very large compared to the atomic cell size.

In order to verify relation (6.1), we shall assume, in addition to the conditions imposed earlier on $\mathfrak{h}$, the condition

$$\text{(iv)} \qquad \lim_{s \to 0} s\mathfrak{h}'(s) = 0.$$

We consider first a sequence $n \mapsto p_n$, such that $p_n \to 0$ as $n \to \infty$, and the corresponding sequence of threshold shear stresses $n \mapsto \bar{\tau}(s_0^t(p_n))$. From the discussion below equation (4.20) and from equation (4.16) we have $0 \leq s_0^t(p_n) \leq p_n/2$, and, by (4.9) and the smoothness of $\mathfrak{h}$, the non-negative numbers $\bar{\tau}(s_0^t(p_n))$ are bounded above by the number $2 \max \psi_1'$ for n sufficiently large. Therefore, we may choose a convergent subsequence $m \mapsto \bar{\tau}(s_0^t(p_m))$. An argument similar to the one used in the Appendix to verify the order of magnitude relation (4.23) may be used here to show that the sequence $m \mapsto \bar{\tau}'(s_0^t(p_m))$ also is convergent. (That argument rests on an additional hypothesis (A.20) made on the constitutive functions φ, ψ_1, and $\mathfrak{h}$ as well as on the orientation of the crystal in the loading device; the appropriateness of the additional hypothesis is discussed in the Appendix.) By (4.15) we have

$$\begin{aligned} p_m \bar{\tau}'(s_0^t(p_m)) &= p_m \mathfrak{h}'(s_0^t(p_m))\psi_1' \left(\frac{1}{p_m} \int_0^{s_0^t(p_m)} \mathfrak{h}(r)dr \right) \\ &+ \mathfrak{h}^2(s_0^t(p_m))\psi_1'' \left(\frac{1}{p_m} \int_0^{s_0^t(p_m)} \mathfrak{h}(r)dr \right) \end{aligned} \tag{6.2}$$

and, because $m \mapsto \bar{\tau}'(s_0^t(p_m))$ converges and $p_m \to 0$ as $m \to \infty$, the left-hand side of (6.2) tends to zero.

Suppose now that $\lim_{m\to\infty} \frac{1}{p_m} \int_0^{s_0^t(p_m)} \mathfrak{h}(r)dr = 0$. Because $\mathfrak{h}' \geq 0$ and $\frac{1}{p_m} \int_0^{s_0^t(p_m)} \mathfrak{h}(r)dr < \frac{1}{2}$, the first term on the right-hand side of (6.2) is non-negative for every m, and the second term tends to $\psi_1''(0) > 0$. This contradicts the fact that the right-hand side of (6.2) tends to zero, and we conclude *not*-$(\lim_{m\to\infty} \frac{1}{p_m} \int_0^{s_0^t(p_m)} \mathfrak{h}(r)dr = 0)$. We note also that, because $\mathfrak{h}(s) \to 1$ as $s \to 0$, $\lim_{m\to\infty} \frac{1}{s_0^t(p_m)} \int_0^{s_0^t(p_m)} \mathfrak{h}(r)dr = 1$ and, therefore:

$$\textit{not-}\left(\lim_{m\to\infty}\frac{1}{p_m}\int_0^{s_0^t(p_m)}\mathfrak{h}(r)dr=0\right)\ \text{if and only if}\ \textit{not-}\left(\lim_{m\to\infty}\frac{s_0^t(p_m)}{p_m}=0\right),$$

so that the truth of the first assertion *not-*$(\lim_{m\to\infty}\frac{1}{p_m}\int_0^{s_0^t(p_m)}\mathfrak{h}(r)dr=0)$, just established above, establishes now the truth of the second: *not-*$(\lim_{m\to\infty}\frac{s_0^t(p_m)}{p_m}=0)$. Because, as we already pointed out, each term of the sequence $n\mapsto s_0^t(p_n)$ is bounded above by $p_n/2$, we may choose a subsequence $j\mapsto s_0^t(p_j)$ and a positive constant C such that $C<\frac{s_0^t(p_j)}{p_j}<\frac{1}{2}$ for all j. When the first term on the right-hand side of (6.2) is multiplied and divided by $s_0^t(p_j)$, we find for all j that

$$\begin{aligned} p_j\bar{\tau}'(s_0^t(p_j)) &= \frac{p_j}{s_0^t(p_j)}s_0^t(p_j)\mathfrak{h}'(s_0^t(p_j))\psi_1'\left(\frac{1}{p_j}\int_0^{s_0^t(p_j)}\mathfrak{h}(r)dr\right)\\ &+ \mathfrak{h}^2(s_0^t(p_j))\psi_1''\left(\frac{1}{p_j}\int_0^{s_0^t(p_j)}\mathfrak{h}(r)dr\right) \end{aligned} \tag{6.3}$$

with $2<\frac{p_j}{s_0^t(p_j)}<\frac{1}{C}$. By assumption (iv) the first term on the right-hand side of (6.3) tends to zero as j tends to infinity. As we already pointed out, $p_j\bar{\tau}'(s_0^t(p_j))$ also tends to zero, so that the second term on the right-hand side also tends to zero, and, consequently,

$$\lim_{j\to\infty}\psi_1''\left(\frac{s_0^t(p_j)}{p_j}\right)=0. \tag{6.4}$$

The inequality $C<\frac{s_0^t(p_j)}{p_j}<\frac{1}{2}$, the assumptions (i) and (ii) introduced in [10] (here made on the functions φ and $s\mapsto p\psi_1(\frac{s}{p})$), and the relation (6.4) together imply

$$\lim_{j\to\infty}\frac{s_0^t(p_j)}{p_j}=\frac{1}{4}. \tag{6.5}$$

By formula (4.9) for $\bar{\tau}(s)$, it follows that

$$\lim_{j\to\infty}\bar{\tau}(s_0^t(p_j))=\psi_1'(\tfrac{1}{4}). \tag{6.6}$$

and the desired result follows by noting that $\psi_1'(\frac{1}{4})=\max\psi_1'$.

7. THE ENVELOPE OF THE CONSTITUTIVE CURVE, FLOW STRESS, AND HARDENING RESPONSE

Equations (4.8), (4.9) provide a parametric description of the constitutive curve in the $\mu-\tau$ plane with the slip s as parameter and with $p=\hat{d}(0)^{-1}$ fixed. The detailed structure of the

constitutive curve in relation to the family of load–orientation curves parameterized by the load f was shown in Section 5 to lead to the "staircase" features of the loading response of a crystal that are observed in experiments. In this section, we derive the equation of the envelope of the family of fundamental branches of constitutive curves obtained by letting p vary, and we discuss the relationship between the envelope, a constitutive quantity, and the predicted staircase loading response of the crystal in Taylor's soft device.

Here we wish to obtain the equation of the envelope of the fundamental branches of the constitutive curve with respect to p, for $\mu \geq 0$ and $\tau \geq 0$. Elementary arguments in analysis show that the relation

$$\frac{\partial}{\partial p}\left(\psi_1'(\frac{1}{p}\int_0^{\mu-\gamma} \mathfrak{h}(s)ds)\right) = 0, \tag{7.1}$$

together with (4.8), (4.9), characterizes the envelope of the family of constitutive curves. Thus, for a given integer j and a given slip s in the fundamental interval I_j, a value $p_j^e(s)$ of p determines a point $(\mu_j^e(s), \tau_j^e(s))$ on the envelope if and only if

$$\psi_1''\left(\frac{1}{p_j^e(s)}\int_0^s \mathfrak{h}(r)dr\right) = 0. \tag{7.2}$$

All of the zeroes of ψ_1'' are of the form $\frac{1}{4}+k$ or $\frac{3}{4}+m$, with k, m non-negative integers, so that the solutions $p_j^e(s)$ of (7.2) must satisfy

$$\frac{1}{p_j^e(s)}\int_0^s \mathfrak{h}(r)dr = \tfrac{1}{4}+k \tag{7.3}$$

or

$$\frac{1}{p_j^e(s)}\int_0^s \mathfrak{h}(r)dr = \tfrac{3}{4}+m. \tag{7.4}$$

Because $s \in I_j := [s_{2j}^0, \mu_{2j+1}^0]$, we have by (4.16)

$$jp_j^e(s) = \int_0^{s_{2j}^0} \mathfrak{h}(r)dr \leq \int_0^s \mathfrak{h}(r)dr \leq \int_0^{\mu_{2j+1}^0} \mathfrak{h}(r)dr = (j+\tfrac{1}{2})p_j^e(s),$$

and, therefore,

$$j \leq \frac{1}{p_j^e(s)}\int_0^s \mathfrak{h}(r)dr \leq j+\tfrac{1}{2}. \tag{7.5}$$

Consequently, (7.4) is not consistent with (7.5), and we conclude that

$$\frac{1}{p_j^e(s)}\int_0^s \mathfrak{h}(r)dr = \tfrac{1}{4}+j, \tag{7.6}$$

and, from the periodicity of ψ_1 and the definition of the initial critical shear stress τ_c in Section 6, that

$$\psi_1' \left(\frac{1}{p_j^e(s)} \int_0^s \mathfrak{h}(r)dr \right) = \psi_1'(\tfrac{1}{4}) = \tau_c. \tag{7.7}$$

Thus, for given s and j, relations (7.7), (4.8), and (4.9), with p replaced by $p_j^e(s)$ in the latter two, yield the following formulae for the macroshear $\mu_j^e(s)$ and the resolved shear stress $\tau_j^e(s)$ of the point $(\mu_j^e(s), \tau_j^e(s))$ on the envelope of the constitutive curve:

$$\begin{aligned} \mu_j^e(s) &= s + (\boldsymbol{\varphi}')^{-1}(\tau_c \mathfrak{h}(s)) \\ \tau_j^e(s) &= \tau_c \mathfrak{h}(s). \end{aligned} \tag{7.8}$$

Because $s \geq 0$ and $j \geq 0$ are arbitrary, the analysis above tells us that a point (μ, τ) in the first quadrant is on the envelope if and only if

$$\begin{aligned} \mu &= \mu^e(s) := s + (\boldsymbol{\varphi}')^{-1}(\tau_c \mathfrak{h}(s)), \\ \tau &= \tau^e(s) := \tau_c \mathfrak{h}(s) \end{aligned} \tag{7.9}$$

for some $s \geq 0$. Eliminating s from equations (7.9) we obtain the desired *equation of the envelope of the constitutive curve*:

$$\mu = \mathfrak{h}^{-1}\left(\frac{\tau}{\tau_c}\right) + (\boldsymbol{\varphi}')^{-1}(\tau) \tag{7.10}$$

(see Figure 6 for the graph of the envelope for aluminum). Since $\mathfrak{h}(s) \geq 1$ for all $s \geq 0$, equations (7.9) tell us that $\tau \geq \tau_c$ and $\mu \geq (\boldsymbol{\varphi}')^{-1}(\tau_c)$ for all points (μ, τ) on the envelope. For the experiments that will be discussed in Section 9, $(\boldsymbol{\varphi}')^{-1}(\tau_c)$ is of the order 10^{-4}, so that the initial point $((\boldsymbol{\varphi}')^{-1}(\tau_c), \tau_c)$ on the envelope (corresponding to $s = 0$ in (7.9)) is very close to the point $(0, \tau_c)$.

In order to determine the relationship between the constitutive curve and the envelope, we let τ_0 be given with τ_0/τ_c in the range of the function $\mathfrak{h}$, we put $\tau = \tau_0$ in both $(7.9)_2$ and (4.2), and set $s^e := \mathfrak{h}^{-1}(\frac{\tau_0}{\tau_c})$. Next, we replace s by s^e in (7.9) and eliminate τ_0 from $(7.9)_2$ and (4.9). We conclude that, if τ_0 and $s \geq 0$ are such that $(\bar{\mu}(s), \tau_0)$ is on the constitutive curve, then

$$\mathfrak{h}(s)\psi_1' \left(\frac{1}{p} \int_0^s \mathfrak{h}(r)dr \right) = \tau_0 = \tau_c \mathfrak{h}(s^e) = (\max \psi_1')\mathfrak{h}(s^e). \tag{7.11}$$

It follows that $\mathfrak{h}(s) \geq \mathfrak{h}(s^e)$, and, by the monotonicity of $\mathfrak{h}$, that $s \geq s^e$. Relations (4.8) and $(7.9)_1$ then yield the inequality $\bar{\mu}(s) \geq \mu^e(s^e)$. Therefore, as a point (μ, τ_0) moves along

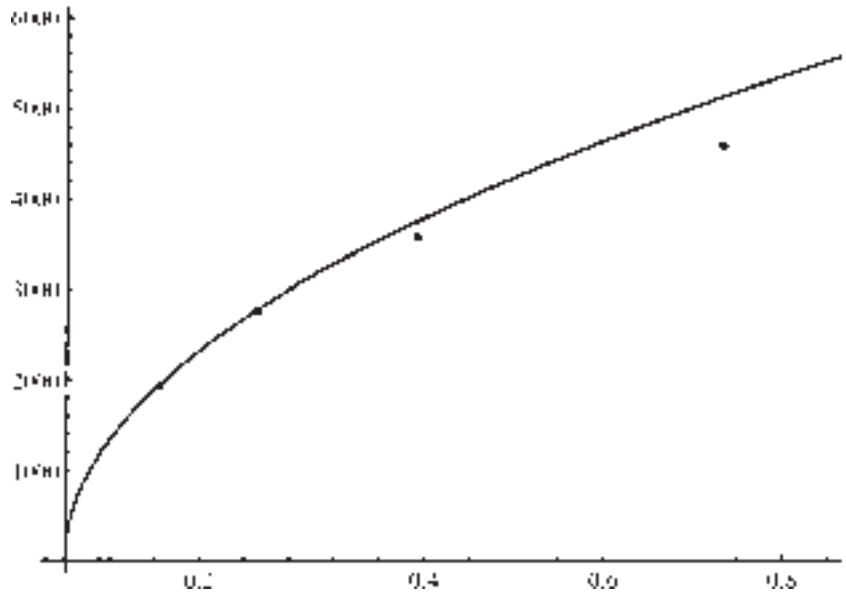

Figure 6. Envelope for aluminum crystal and the (μ, τ) points of Taylor [1, p.213, Table 1].

the line $\tau = \tau_0$, with μ increasing from the value 0, the point $(\mu^e(s^e), \tau_0)$ on the envelope is reached before any points $(\bar{\mu}(s), \tau_0)$ on the constitutive curve. Thus, for $\mu \geq (\varphi')^{-1}(\tau_c)$, points (μ, τ) on the envelope lie on or above the constitutive curve. In conclusion, according to the present theory, *when the crystal is subjected to a monotonic loading program in Taylor's soft device, the attainable points* (μ, τ) *for the crystal lie on or below the envelope of the constitutive curve*. We emphasize that the envelope is determined by the constitutive curve alone, whereas the attainable points depend both on the loading device and the constitutive curve.

The geometry of the load–orientation curves and the constitutive curve is further specified, if we require that for each point $(\mu^e, \tau^e) := (\mu^e(s^e), \tau^e(s^e))$ on the envelope, the slope of the load–orientation curve through (μ^e, τ^e) is less than the slope of the envelope at that point:

$$\hat{\tau}'_{\bar{f}(s^e)}(\mu^e) < \frac{\tau^{e\prime}(s^e)}{\mu^{e\prime}(s^e)}. \tag{7.12}$$

This inequality and the concavity of load–orientation curves tells us that the load–orientation curve through (μ^e, τ^e) must cross the envelope at (μ^e, τ^e) and remain between the envelope and the μ-axis. Because each fundamental branch of the constitutive curve continuously connects the μ-axis and the envelope, *each load–orientation curve must intersect every fundamental branch of the constitutive curve from some point on.*

It is worth noting that each point (μ^e, τ^e) on the envelope may be viewed as a limit of threshold points $(\bar{\mu}(s^t_{2j}), \bar{\tau}(s^t_{2j}))$, where $j \to \infty$ and $p \to 0$ in such a way that $pj \to \mu^e$. This result follows from arguments similar to ones provided in Section 6 (showing that the initial critical resolved shear stress τ_c is the limit of the first threshold resolved shear stress as

$p \to 0$) and in Section 10. Together with the fact that values of p for many crystals are of the order 10^{-4}, this result suggests that there are many threshold points close to the envelope.

The purely constitutive nature of the envelope suggests that it may be used to select a family of two-level shears for the crystal that characterize the "device-independent" loading properties of the crystal. To this end, we note that, for each point $(\mu, \tau) = (\mathfrak{h}^{-1}(\frac{\tau}{\tau_c}) + (\boldsymbol{\varphi}')^{-1}(\tau), \tau)$ on the envelope, a macroshear $\mu^*(\tau)$ and a shear without slip $\gamma^*(\tau)$ can be assigned via the relations

$$\begin{aligned} \gamma^*(\tau) &:= (\boldsymbol{\varphi}')^{-1}(\tau) \\ \mu^*(\tau) &:= \mathfrak{h}^{-1}\left(\frac{\tau}{\tau_c}\right) + (\boldsymbol{\varphi}')^{-1}(\tau). \end{aligned} \tag{7.13}$$

Moreover, the additional assignment

$$s^*(\tau) := \mu^*(\tau) - \gamma^*(\tau) = \mathfrak{h}^{-1}\left(\frac{\tau}{\tau_c}\right) \tag{7.14}$$

associates with each $\tau \geq \tau_c$ the shear due to slip for the crystal corresponding to the point (μ, τ) on the envelope. These assignments can be viewed as constitutive functions $\tau \mapsto (\mu^*(\tau), \gamma^*(\tau))$ and $\tau \mapsto s^*(\tau)$ that assign a two-level shear to each point on the envelope. In view of relations (7.9) and (7.14), we have for all $s \geq 0$

$$\tau = \tau^e(s) = \tau_c \mathfrak{h}(s), \tag{7.15}$$

a relation that determines on the envelope the resolved shear stress τ as a function of the shear due to slip s**.** We call the function $\tau_c \mathfrak{h}$ the *hardening response function of the crystal (for two-level shears)* **,** and we note that $\tau_c \mathfrak{h}$ is determined by the response functions $\mathfrak{h}$ and ψ_1**.** We call the number $\tau_c \mathfrak{h}(s)$ the *flow stress* for the slip s: it depends upon the crystal and the amount of slip s but not upon the particular loading device employed. Our use of this widely employed term [5, 19] is based on the proximity of threshold points to points on the envelope established above.

8. UNLOADING

In Section 5 we gave a detailed description of the loading of a crystal first in the simple case where each fundamental branch of the constitutive curve is a simple curve with exactly one local maximum and at most one point with a vertical tangent and where each fundamental branch and each load–orientation curve either cross exactly twice or intersect at most once. We then outlined a description of loading in the more general case when these restrictions were relaxed. Here, we discuss in less detail the unloading of a crystal first in the simple case and, at the end of the section, in the general case.

We suppose that the crystal has undergone loading, with the load increased monotonically from the value 0 to a value f, and that the attainable point $(\mu,\tau) = (\bar{\mu}(s^c_{2\,j}),\bar{\tau}(s^c_{2\,j}))$ on the jth-fundamental branch has been reached via the staircase response described in Section 5. Assume now that the load is decreased monotonically to zero. The fact that the load–orientation curve through the attainable point $(\bar{\mu}(s^c_{2\,j}),\bar{\tau}(s^c_{2\,j}))$ crosses the jth-fundamental branch twice and the fact that load–orientation curves for different loads cannot cross imply that the points $(\bar{\mu}(s),\bar{\tau}(s))$ for $s \in [s^0_{2\,j}, s^c_{2\,j}]$ are metastable. Therefore, it is consistent with decreasing loads to have the slip decrease from its maximum value $s^c_{2\,j}$ to the value $s^0_{2\,j}$ and, correspondingly, to have the metastable points $(\bar{\mu}(s),\bar{\tau}(s))$ follow the jth-fundamental branch until the point $(\bar{\mu}(s^0_{2\,j}),\bar{\tau}(s^0_{2\,j})) = (s^0_{2\,j},0)$ on the μ-axis is reached. As is customary, we call this process *unloading*, and the calculation in (4.25) shows that the shearing of the crystal during unloading involves no dissipation. Hence, the energy function (2.14) is compatible both with loading along a staircase locus as described in Section 5 and with unloading.

If the force again is increased, the jth-fundamental branch can be retraced up to the threshold point $(\bar{\mu}(s^t_{2\,j}),\bar{\tau}(s^t_{2\,j}))$, again without dissipation. However, experiments [20] on the behavior of single crystals under reloading indicate that the upward retracing of the jth-fundamental branch actually may cease before the threshold slip $s^t_{2\,j}$ is reached. Thus, while the simple case described here adequately describes the behavior of single crystals under initial loading and unloading, the assumptions underlying this case do not capture a change in the threshold slip upon reloading.

If one examines the detailed process of unloading when these assumptions are relaxed, one finds that the points $(\mu.\tau)$ can undergo dissipative jumps corresponding to flat portions of a staircase locus. However, the total dissipation during unloading turns out to be of the order $O(p^2)$, and the role of dissipation during unloading can be expected to be negligible in the general case.

9. APPLICATION TO ALUMINUM CRYSTALS

An application of our theory to aluminum single crystals can be made by using data from Taylor's experiments on slip and hardening in single crystals [1]. To do so, we make particular choices for the constitutive functions φ, ψ_1, and $\mathfrak{h}$ appearing in (2.14). Specifically, we assume that the lattice energy $\varphi(\gamma)$ away from slip bands is quadratic with shear modulus k and that the energy due to slip $\psi_1(s)$ takes a form similar to that suggested in [10]:

$$\varphi(\gamma) = \frac{1}{2}k\gamma^2 \quad \text{and} \quad \psi_1(s) = \frac{\tau_c}{2\pi}(1-\cos(2\pi s)). \tag{9.1}$$

The coefficient τ_c equals $\psi_1'(\frac{1}{4})$ and, therefore, is the inital critical resolved shear stress defined in Section 6. The numbers k and τ_c are characteristic properties of the material: for aluminum, we can take k in the range $7.3 \times 10^5 - 8.5 \times 10^5$ psi ([15], p.533), and $\tau_c = 2.93 \times 10^2$ psi ([15], p. 347). (These values of k and $\tau_c = \psi_1'(\frac{1}{4})$ are consistent with relation (A.20) given in the Appendix and employed in the verification of the formula (6.1).) There is general agreement in the literature that, during monotonic loading programs

covering a wide range of shears, square-root hardening behavior occurs [1, 3, 5, 6, 16], and we take

$$\mathfrak{h}(r) := 1 + ar^{\frac{1}{2}}, \quad r \geq 0, \tag{9.2}$$

where a is a dimensionless parameter. Here we take $a \approx 195.19$ to be the smallest number for which the points determined in Taylor's experiments ([1], p.213, Table 1), all lie on or below the envelope given in (7.10) with $\mathfrak{h}$ of the assumed form (9.2) and φ as in (9.1). In Figure 6, the envelope of the constitutive curve is depicted together with four points (μ, τ) calculated by Taylor from his tensile test ([1], p.213, Table 1). The formula (9.2) and the definition (2.10) yield the formulas

$$\hat{d}(s) = \frac{\hat{d}(0)}{s} \int_0^s \mathfrak{h}(r)dr = \hat{d}(0)(1 + \tfrac{2}{3}as^{\frac{1}{2}}) \tag{9.3}$$

for the relative separation of active slip bands as a function of s and initial separation $\hat{d}(0)$.

The relation (9.3) implies an increase in the separation of *active* slip-bands in response to an increase in the amount of shear s. This prediction is not in conflict with observations in aluminum crystals that the separation of all slip bands, *active* and *inactive*, decreases with s (see [13], Section 1 for references to such experimental observations).

For this consitutive description of an aluminum single crystal, the inequality (7.12) used in the analysis of the envelope in Section 7, now written in the detailed form

$$\tau^e \frac{\hat{\tau}_1'(\mu^e)}{\hat{\tau}_1(\mu^e)} < \frac{\varphi''(s^e)\tau_c\mathfrak{h}'(s^e)}{\varphi''(s^e) + \tau_c\mathfrak{h}'(s^e)}, \tag{9.4}$$

will be satisfied if the simpler inequality

$$C\tau_c(1 + a\sqrt{\mu^e}) < k \tag{9.5}$$

holds. Here, $k = \min\varphi'' > 0$ and the positive number C is given by the fraction containing θ_0 and η_0 appearing as the last member in the inequality (A.17). Using the values $\theta_0 = 41.9°$, $\eta_0 = 23°$ above Table 1, p. 213 in [1], it is easy to check that (9.5) is satisfied when the macroshear μ^e is between 0 and 1.

APPENDIX

To verify (4.21), we use relation (4.16) to write

$$p = \int_{\mu^0_{2j}}^{\mu^0_{2j+1}} \mathfrak{h}(r)dr = \int_{s^0_{2j}}^{\mu^0_{2j+1}} \mathfrak{h}(r)dr \tag{A.1}$$

and the fact that $\mathfrak{h}$ is non-decreasing with $\mathfrak{h}(0) = 1$ to conclude that

$$\mu^0_{2j+1} - s^0_{2j} \leq p \leq (\mu^0_{2j+1} - s^0_{2j})\mathfrak{h}(\mu^0_{2j+1}). \tag{A.2}$$

Similarly,

$$\mu^0_{2j+1} = \int_0^{\mu^0_{2j+1}} dr \le \int_0^{\mu^0_{2j+1}} \mathfrak{h}(r)dr = (j+\tfrac{1}{2})p, \tag{A.3}$$

so that $\mathfrak{h}(\mu^0_{2j+1}) \le \mathfrak{h}((j+\frac{1}{2})p)$, and (10.2) now yields

$$\frac{p}{\mathfrak{h}((j+\frac{1}{2})p)} \le \mu^0_{2j+1} - s^0_{2j} \le p. \tag{A.4}$$

This establishes relation (4.21), and (4.22) is verified in a similar way starting from (4.17).

We consider now the behavior of s^0_{2j}, μ^0_{2j+1}, and s^q_{2j} as p tends to zero and j tends to infinity in such a way that the product jp has a finite limit $\ell \ge 0$. It follows from (4.16) and the properties of $\mathfrak{h}$ that μ^0_{2j+1} also has a limit $s_\ell \ge 0$. Relation (A.4) now implies:

$$\lim_{p\to 0}\lim_{jp\to\ell} \mu^0_{2j+1} = \lim_{p\to 0}\lim_{jp\to\ell} s^0_{2j} = s_\ell, \tag{A.5}$$

and, in a similar fashion, we may conclude that

$$\lim_{p\to 0}\lim_{jp\to\ell} s^q_{2j} = s_\ell. \tag{A.6}$$

These arguments also tell us that the absolute value of the $O(p)$ terms in (4.21) and (4.22) can be bounded above by p and by $\frac{p}{4}$, respectively.

To prove (4.23) and (4.24), we first verify the following result: *if* $(p,j) \mapsto s(p,j) \in [s^0_{2j}, \mu^0_{2j+1}]$ *is a family of slips for which* $(p,j) \mapsto \bar{\tau}'(s(p,j))$ *and* $(p,j) \mapsto \mathfrak{h}'(s(p,j))$ *are bounded, then there exists a positive constant* C *such that*

$$\left|s(p,j) - s^q_{2j}\right| \le Cp^2 \tag{A.7}$$

as $p \to 0$ *and* $j \to \infty$ *with* $jp \to \ell \ge 0$. Indeed, by (4.16), (4.17), and the bound on $s(p,j)$ given through (A.3), we have that

$$\left|\frac{1}{p}\int_{s^q_{2j}}^{s(p,j)} \mathfrak{h}(r)dr\right| \le \frac{1}{4} \tag{A.8}$$

and, by (4.15) and the smoothness and periodicity of ψ_1, that

$$\begin{aligned}\bar{\tau}'(s(p,j)) &= \mathfrak{h}'(s(p,j))\psi_1'\left(\tfrac{1}{p}\int_0^{s(p,j)} \mathfrak{h}(r)dr\right)\\ &+ \tfrac{\mathfrak{h}^2(s(p,j))}{p}\psi_1''\left(j+\tfrac{1}{4}+\tfrac{1}{p}\int_{s^q_{2j}}^{s(p,j)} \mathfrak{h}(r)dr\right)\end{aligned}$$

$$
\begin{aligned}
&= \mathfrak{h}'(s(p,j))\psi_1'\left(\tfrac{1}{p}\int_0^{s(p,j)} \mathfrak{h}(r)dr\right)\\
&+ \tfrac{\mathfrak{h}^2(s(p,j))}{p}\psi_1''\left(\tfrac{1}{4}+\tfrac{1}{p}\int_{s^q_{2\,j}}^{s(p,j)} \mathfrak{h}(r)dr\right)\\
&= \mathfrak{h}'(s(p,j))\psi_1'\left(\tfrac{1}{p}\int_0^{s(p,j)} \mathfrak{h}(r)dr\right)\\
&+ \tfrac{\mathfrak{h}^2(s(p,j))}{p}\left(\psi_1''(\tfrac{1}{4})+\psi_1'''(\lambda\ (p,j))\tfrac{1}{p}\int_{s^q_{2\,j}}^{s(p,j)} \mathfrak{h}(r)dr\right). \qquad \text{(A.9)}
\end{aligned}
$$

In (A.9), $\lambda\ (p,j)$ is between $\frac{1}{4}$ and $\frac{1}{4}+\frac{1}{p}\int_{s^q_{2\,j}}^{s(p,j)}\mathfrak{h}(r)dr$ and, therefore, by (A.8), is in the interval $[0,\frac{1}{2}]$. Moreover, by (A.5), (A.6), and the assumed bounds $s(p,j)\in[s^0_{2\,j},\mu^0_{2\,j+1}]$,

$$\lim_{p\to 0}\lim_{jp\to\ell} s(p,j)=s_\ell. \qquad \text{(A.10)}$$

Because $\mathfrak{h}'(s(p,j))$ and $\bar{\tau}'(s(p,j))$ are bounded, the assumptions (i), (ii), and (iii) on φ and ψ (see the paragraph preceding (4.20)) together with the first two relations in (A.9) tell us that $\psi_1''(\frac{1}{4}+\frac{1}{p}\int_{s^q_{2\,j}}^{s(p,j)}\mathfrak{h}(r)dr)$ tends to zero. Noting that $\frac{1}{4}$ is the only zero of ψ_1'' in the interval $[0,\frac{1}{2}]$, we conclude that $\frac{1}{p}\int_{s^q_{2\,j}}^{s(p,j)}\mathfrak{h}(r)dr\to 0$ as $p\to 0$ with $jp\to\ell$. Because $\lambda\ (p,j)$ is between $\frac{1}{4}$ and $\frac{1}{4}+\frac{1}{p}\int_{s^q_{2\,j}}^{s(p,j)}\mathfrak{h}(r)dr$, we have

$$\lim_{p\to 0}\lim_{jp\to\ell}\lambda\ (p,j)=\frac{1}{4}. \qquad \text{(A.11)}$$

Rewriting the last relation in (A.9) as

$$\bar{\tau}'(s(p,j))=\mathfrak{h}'(s(p,j))\psi_1'\left(\tfrac{1}{p}\int_0^{s(p,j)}\mathfrak{h}(r)dr\right)+\tfrac{\mathfrak{h}^2(s(p,j))}{p}\psi_1'''(\lambda\ (p,j))\tfrac{1}{p}\int_{s^q_{2\,j}}^{s(p,j)}\mathfrak{h}(r)dr$$

and using the boundedness of $\mathfrak{h}'(s(p,j))$ and $\bar{\tau}'(s(p,j))$, we conclude that the second term on the right-hand side of this relation is bounded. Moreover, $\mathfrak{h}^2(s(p,j))\ \psi_1'''(\lambda\ (p,j))$ is bounded away from zero, so that there exists a positive constant $\bar{C}$ independent of p and j such that

$$\left|\int_{s^q_{2\,j}}^{s(p,j)}\mathfrak{h}(r)dr\right|\le\bar{C}p^2. \qquad \text{(A.12)}$$

The desired relation (A.7) follows from (A.12) and the assumed properties of $\mathfrak{h}$.

To verify (4.24), we put $s(p,j) := s^m_{2j}$ and note that $s^m_{2j} \in [s^q_{2j}, \mu^0_{2j+1}] \subset [s^0_{2j}, \mu^0_{2j+1}]$, and $\bar\tau'(s^m_{2j}) = 0$ for all p and j. Hence, if $\mathfrak{h}$ is continuously differentiable in a neighborhood of s_ℓ, then there exists $C > 0$ such that

$$\left| s^m_{2j} - s^q_{2j} \right| \le Cp^2 \tag{A.13}$$

as $p \to 0$ with $jp \to \ell$, and (4.24) is established.

To verify (4.23), we put $s(p,j) := s^t_{2j}$, and we recall that $s^t_{2j} \in (s^0_{2j}, s^m_{2j}) \subset [s^0_{2j}, \mu^0_{2j+1}]$. Moreover, by (4.10), (4.12), (4.13), and (4.15), we have

$$\begin{aligned}
& \bar\tau'(s^t_{2j}) \left(\boldsymbol{\varphi}'' \left((\boldsymbol{\varphi}')^{-1}(\bar\tau(s^t_{2j})) \right) \right. \\
- \; & \left. \frac{\bar\tau(s^t_{2j})}{\hat\tau_1\left(s^t_{2j} + (\boldsymbol{\varphi}')^{-1}(\bar\tau(s^t_{2j}))\right)} \hat\tau_1' \left(s^t_{2j} + (\boldsymbol{\varphi}')^{-1}(\bar\tau(s^t_{2j})) \right) \right) \\
= \; & \boldsymbol{\varphi}'' \left((\boldsymbol{\varphi}')^{-1}(\bar\tau(s^t_{2j})) \right) \frac{\bar\tau(s^t_{2j})}{\hat\tau_1\left(s^t_{2j} + (\boldsymbol{\varphi}')^{-1}(\bar\tau(s^t_{2j}))\right)} \\
\times \; & \hat\tau_1' \left(s^t_{2j} + (\boldsymbol{\varphi}')^{-1}(\bar\tau(s^t_{2j})) \right) .
\end{aligned} \tag{A.14}$$

We wish to use (A.14) to show that the family $(p,j) \mapsto \bar\tau'(s^t_{2j})$ is bounded, and, to this end, it is sufficient to show that the coefficient of $\bar\tau'(s^t_{2j})$ is bounded away from zero. More specifically, it will suffice to show that there exist two numbers A and B satisfying

$$\frac{\hat\tau_1'\left(s^t_{2j} + (\boldsymbol{\varphi}')^{-1}(\bar\tau(s^t_{2j}))\right)}{\hat\tau_1\left(s^t_{2j} + (\boldsymbol{\varphi}')^{-1}(\bar\tau(s^t_{2j}))\right)} \bar\tau(s^t_{2j}) < A < B < \boldsymbol{\varphi}'' \left((\boldsymbol{\varphi}')^{-1}(\bar\tau(s^t_{2j})) \right) \tag{A.15}$$

for all p and j. From relation (4.9) and the monotonicity of $\mathfrak{h}$, we obtain the inequality

$$\bar\tau(s^t_{2j}) < (\max \psi_1')\mathfrak{h}(s_\ell + 1) \tag{A.16}$$

for p near zero and j sufficiently large. In addition the formula (3.13) implies

$$\begin{aligned}
& \frac{\hat\tau_1'\left(s^t_{2j} + (\boldsymbol{\varphi}')^{-1}(\bar\tau(s^t_{2j}))\right)}{\hat\tau_1\left(s^t_{2j} + (\boldsymbol{\varphi}')^{-1}(\bar\tau(s^t_{2j}))\right)} \\
\le \; & \frac{1 + \tan^2\theta_0 \sin^2\eta_0}{(\bar\mu(s^t_{2j}) + \tan\theta_0 \cos\eta_0)\left(1 + \tan^2\theta_0 \sin^2\eta_0 + \left(\bar\mu(s^t_{2j}) + \tan\theta_0\cos\eta_0\right)^2\right)^{\frac{3}{2}}} \\
\le \; & \frac{1 + \tan^2\theta_0 \sin^2\eta_0}{\tan\theta_0 \cos\eta_0 (1 + \tan^2\theta_0)^{\frac{3}{2}}}
\end{aligned} \tag{A.17}$$

and, according to (A.16) and (A.17), we put

$$A := (\max \psi_1')\mathfrak{h}(s_\ell + 1)\frac{1+\tan^2\theta_0 \sin^2\eta_0}{\tan\theta_0 \cos\eta_0 (1+\tan^2\theta_0)^{\frac{3}{2}}}. \tag{A.18}$$

Moreover, the assumption (i) on φ permits us to put

$$B := k = \min \varphi''. \tag{A.19}$$

The desired relation (A.15) follows from (A.16)–(A.19), provided that we require $A < B$ or, equivalently,

$$\frac{(\max \psi_1')\mathfrak{h}(s_\ell + 1)}{k} < \frac{\tan\theta_0 \cos\eta_0 (1+\tan^2\theta_0)^{\frac{3}{2}}}{1+\tan^2\theta_0 \sin^2\eta_0}. \tag{A.20}$$

In Section 9 we refer to experimental data for which the left and right members of (A.20) are of the order 10^{-3} and 1, respectively.

We summarize the result of the above consideration as follows: *if* $\mathfrak{h}$ *is continuously differentiable in a neighborhood of* s_ℓ *and if (A.20) holds, then there exists* $\tilde{C} > 0$ *independent of* j *and* p *such that*

$$\left| s^t_{2j} - s^q_{2j} \right| \leq \tilde{C}p^2 \qquad \text{as } p \to 0 \text{ with } jp \to \ell, \tag{A.21}$$

and this implies (4.23).

Acknowledgments: The authors acknowledge the National Science Foundation Grant DMS 9703863 for support provided to D. R. Owen. They also acknowledge the Gruppo Nazionale per la Fisica Matematica and V. Boffi for financial support provided to L. Deseri through a joint program with the Center for Nonlinear Analysis, Department of Mathematical Sciences, Carnegie Mellon, as well as the Ministero Dell Universita e per la Ricerca Scientifica e Tecnologica through the grants: (i) 60% Prof. Del Piero, 1998, and (ii) Modelli matematici per la scienza dei materiali (Co.Fin. 1998). Subsequent support for L. Deseri was provided by the Center for Nonlinear Analysis, Department of Mathematical Sciences, Carnegie Mellon.

We are indebeted to L. Truskinovsky for reminding us of the fact that increasing the separation of slip bands can increase the frequency of oscillations of the free energy due to slip. We also acknowledge technical help provided by R. Rizzieri in preparing the figures.

NOTE

1. To whom correspondence should be addressed.

REFERENCES

[1] Taylor, G. I.: *The Scientific Papers of Sir Geoffrey Ingram Taylor*, vol I, Mechanics of Solids, ed. G. K. Batchelor, Cambridge University Press, 1958.

[2] Hill, R.: *The Mathematical Theory of Plasticity*, Oxford University Press, 1950.

[3] Rice, J. R.: Inelastic constitutive relations for solids: an internal variable theory and its application to metal plasticity. *Journal of the Mechanics and Physics of Solids*, 19, 433–455 (1971).

[4] Rice, J. R.: Continuum Mechanics and Thermodynamics of Plasticity in Relation to Microscale Deformation Mechanisms, in *Constitutive Equations in Plasticity*, pp. 23–79, ed. A. S. Argon, Cambridge MA, MIT Press, 1975.

[5] Havner, K. S.: *Finite Plastic Deformation of Crystalline Solids*, Cambridge University Press, 1992.

[6] Ortiz, M. and Repetto, E. A.: Nonconvex energy minimization and dislocation structures in ductile single crystals. *Journal of the Mechanics and Physics of Solids*, 47 (2), 397–462 (1999).

[7] Del Piero, G. and Owen, D. R.: Structured deformations of continua. *Archive for Rational Mechanics and Analysis*, 124, 99–155 (1993).

[8] Del Piero, G. and Owen., D. R.: Integral-gradient formulae for structured deformations. *Archive for Rational Mechanics and Analysis*, 131, 121–138 (1995).

[9] Owen, D. R.: Structured deformations and the refinements of balance laws induced by microslip. *International Journal of Plasticity*, 14, 289–299 (1998).

[10] Choksi, R., Del Piero, G., Fonseca, I. and Owen, D. R.: Structured deformations as energy minimizers in models of fracture and hysteresis. *Mathematics and Mechanics of Solids*, 4, 321–356 (1999).

[11] Deseri, L. and Owen, D. R.: Invertible structured deformations and the geometry of multiple slip in single crystals. *International Journal of Plasticity*, forthcoming. Research Report No. 00-CNA-002, Center for Nonlinear Analysis, Carnegie Mellon University, Pittsburgh, PA.

[12] Choksi, R. and Fonseca, I.: Bulk and interfacial energy densitites for structured deformations of continua. *Archive for Rational Mechanics and Analysis*, 138, 37–103 (1997).

[13] Deseri, L. and Owen, D.R.: Active slip-band separation and the energetics of slip in single crystals. *International Journal of Plasticity* 16, 1411–1418 (2000).

[14] Salama, A., Shaikh, F. and Roberts, J.M.: Microstrain and electron micrographics slip studies of ordered and disordered Cu_3Au, *Acta Metallurgica*, 19, 395–404 (1971).

[15] Barret, C. S.: *Structure of Metals*, Second Ed., McGraw-Hill, New York, Toronto, London, 1952.

[16] Bell, J. F.: *The Physics of Large Deformation of Crystalline Solids*, Springer Tracts in Natural Philosophy, 14, Springer, Berlin, 1968.

[17] Bell, J. F.: The Experimental Foundation of Solid Mechanics, in *Handbuch der Physik*, Vol. VIa/1, ed. C. Truesdell, pp 1–813, Springer, Berlin, 1973.

[18] Sharpe, W. N.: The Portevin-le Chatelier effect in aluminium single crystals and polycrystals, *Journal of the Mechanics and Physics of Solids*, 14, 187–202 (1966).

[19] Gilman, J. J.: *Micromechanics of Flow in Solids*, McGraw-Hill, New York, Toronto, London, 1969.

[20] Buckley, S. N. and Entwistle, K. M.: The Baushinger effect in super-pure aluminum single crystals and polycrystals. *Acta Metallurgica*, 4, 352–361 (1956).